ACS OMEGA

Open Access



http://pubs.acs.org/journal/acsodf

Article

# From Mono- to Polynuclear 2-(Diphenylphosphino)pyridine-Based Cu(I) and Ag(I) Complexes: Synthesis, Structural Characterization, and DFT Calculations

Jasmin M. Busch, Florian R. Rehak, Valentina Ferraro, Martin Nieger, Marianna Kemell, Olaf Fuhr, Wim Klopper,* and Stefan Bräse*

Cite This: *ACS Omega* 2024, 9, 2220−2233

Read Online

ACCESS | Metrics & More | Article Recommendations | Supporting Information

**ABSTRACT:** A series of monometallic Ag(I) and Cu(I) halide complexes bearing 2-(diphenylphosphino)pyridine (PyrPhos, L) as a ligand were synthesized and spectroscopically characterized. The structure of most of the derivatives was unambiguously established by X-ray diffraction analysis, revealing the formation of mono-, di-, and tetranuclear complexes having general formulas $\mathbf{MXL_3}$ (M = Cu, X = Cl, Br; M = Ag, X = Cl, Br, I), $\mathbf{Ag_2X_2L_3}$ (X = Cl, Br), and $\mathbf{Ag_4X_4L_4}$ (X = Cl, Br, I). The Ag(I) species were compared to the corresponding Cu(I) analogues from a structural point of view. The formation of Cu(I)/Ag(I) heterobimetallic complexes $\mathbf{MM'X_2L_3}$ (M/M′ = Cu, Ag; X = Cl, Br, I) was also investigated. The X-ray structure of the bromo-derivatives revealed the formation of two possible $\mathbf{MM'Br_2L_3}$ complexes with Cu/Ag ratios, respectively, of 7:1 and 1:7. The ratio between Cu and Ag was studied by scanning electron microscopy−energy-dispersive X-ray analysis (SEM−EDX) measurements. The structure of the binuclear homo- and heterometallic derivatives was investigated using density functional theory (DFT) calculations, revealing the tendency of the PyrPhos ligands not to maintain the bridging motif in the presence of Ag(I) as the metal center.

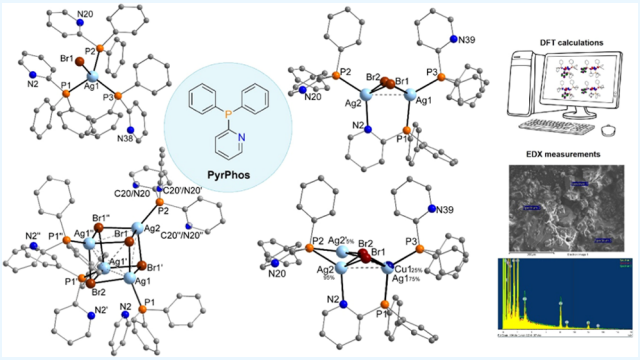


## 1. INTRODUCTION

Mono- and polynuclear Cu(I) complexes exhibiting thermally activated delayed fluorescence (TADF) were deeply investigated for their potential application to organic light-emitting diodes (OLEDs). This peculiar feature allows us to harvest both singlet (25%) and triplet excitons (75%) due to the small energy gap ($\Delta E < 1500\ cm^{-1}$) between the first singlet and triplet states ($S_1$ and $T_1$), leading to a potential 100% of internal quantum efficiency (IQE).[1−8] Besides Cu(I) complexes,[9−13] Ag(I),[14−17] Au(III),[18−23] and Zn(II) derivatives,[24−26] as well as pure organic molecules, were deeply studied for such purposes.[6,27−29] In this context, NP ligands were employed to prepare multinuclear complexes after the pioneering studies conducted by Yersin and co-workers using 2-(diphenylphosphino)pyridine (PyrPhos).[30−32] The possible coordination both *via* the phosphorus and the nitrogen atoms, together with the different stoichiometries for the Cu(I) halides, determines a wide variety of architectures that can be potentially obtained.[32,33] In addition, the modification of the fragments around the phosphorus atom, for instance, substituting the pyridine fragment with a pyrimidine or a pyridazine[34,35] or introducing other heterocycles instead of the phenyl groups,[36−39] permitted one to synthesize a wide library of NP ligands. It is worth mentioning that in the latter case, the first example of a triple bridging ligand was recently reported by Artem'ev and co-workers using tris[2-(2-pyridyl)ethyl]-phosphine.[40]

Other possible modifications in the skeleton of the NP ligand involve the use of the corresponding phosphine oxides[41−43] or arsine derivatives.[44,45] In both cases, properties such as TADF and X-ray radioluminescence were detected in the derived Cu(I) complexes.

As concerns Ag(I) complexes, the corresponding analogues with NP ligands are much less investigated. Only a few examples were reported in the literature, for instance, with tris(2-pyridyl)phosphine,[46] diphenyl(2-pyrazyl)phosphine,[47] and tris(2-pyridyl)phosphine oxide.[48]

Given the interest toward the synthesis of luminescent Cu(I) complexes with halides and NP ligands,[30,32,49−56] we deemed it interesting to study their corresponding Ag(I)

**Received:** August 6, 2023
**Revised:** October 21, 2023
**Accepted:** October 25, 2023
**Published:** January 4, 2024

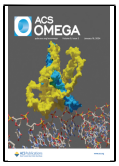

derivatives and the formation of heterobimetallic complexes having the general formula $\mathbf{MM'X_2L_3}$ (M/M′ = Cu, Ag; X = Cl, Br, I; L = PyrPhos). It is worth mentioning that the presence of Van der Waals interactions between closed-shell $d^{10}$ ions proved to influence the photophysical properties of the corresponding metal complexes as it was previously reported for Au(I)−Ag(I), Au(I)−Cu(I), and Ag(I)−Cu(I) derivatives.[57−61] The ratio between Cu(I) and Ag(I) was investigated using scanning electron microscopy in combination with energy-dispersive X-ray spectroscopy (SEM−EDX) measurements. To the best of our knowledge, only $\mathbf{Ag_2Cl_2L_3}$ and $\mathbf{Ag_4Cl_4L_4}$ were previously reported in the literature, but the position of the nitrogen atoms of the PyrPhos ligands was not properly assigned.[62,63] On the other hand, it is worth mentioning that homoleptic Ag(I) complexes with PyrPhos behaving as monodentate or bridging ligand were reported in the past.[64]

## 2. EXPERIMENTAL SECTION

**2.1. General Remarks.** The solvents were purchased from Fisher Scientific if not stated otherwise. Dichloromethane and acetonitrile for the complex synthesis were dried with the solvent purification system (SPS) from MBraun (model MB-SPS-800) and were degassed with argon before usage (5 and 15 min, respectively). The precipitation of the Cu(I) complexes was performed with *n*-pentane purchased from Merck. 2-(Diphenylphosphino)pyridine (PyrPhos) was purchased from abcr together with CuBr, AgCl, and AgI (99.9%). CuI (99.999% trace metal basis) and CuCl (≥99.99% trace metal basis) were purchased from Merck, while AgBr (99.9%) was purchased from Fisher Scientific. All chemicals were used without any further purification. The heteronuclear NMR spectra of the Cu(I) and Ag(I) PyrPhos complexes were recorded in degassed DMSO-$d_6$ or $CDCl_3$ purchased from Euriso-Top. All reactions were carried out under Schlenk techniques under an Ar atmosphere, and the reaction mixtures were stirred in the dark. The synthesis and analytical data of the dinuclear Cu(I) PyrPhos complexes $\mathbf{Cu_2X_2L_3}$ (with X = Cl, Br, I) were reproduced according to the literature procedure.[65]

General information concerning NMR, mass spectrometry, IR, and elemental analyses, as well as melting points, solubility studies, SEM−EDX, and single-crystal X-ray diffraction (XRD) analyses, is detailed in the Supporting Information. Additional information on the experimental procedure is available via the repository Chemotion.[66]

**2.2. General Procedure for the Synthesis of [CuX(PyrPhos)$_3$] (CuXL$_3$, X = Cl, Br) Complexes.** PyrPhos (1.00 g, 3.80 mmol, 3.00 equiv) and CuX (0.125 g for CuCl and 0.182 g for CuBr, 1.27 mmol, 1.00 equiv) were suspended in 15 mL of dichloromethane. The reaction mixture was degassed with Ar for 5 min and was stirred for 24 h at 25 °C. The volume of the clear and yellow solution was reduced to 10 mL under reduced pressure. The solution was added dropwise to 250 mL of *n*-pentane. The precipitate was filtered off, washed with *n*-pentane (4 × 25 mL), and dried *in vacuo*. Complexes $\mathbf{CuClL_3}$ and $\mathbf{CuBrL_3}$ were, respectively, obtained as off-white and pale yellow powders and crystallized from acetonitrile.

*2.2.1. CuClL$_3$.* Yield: 0.775 g (69%). $^1$H NMR (400 MHz, DMSO-$d_6$, ppm) $\delta$ = 8.61 (bs, 3H, $H_{L(Pyr)}$), 7.69 (t, $J_{HH}$ = 7.4 Hz, 3H, $H_{L(Pyr)}$), 7.41−7.28 (m, 36H, $H_{L(Pyr)}$, $H_{L(Ph)}$). $^{31}$P{$^1$H} NMR (162 MHz, DMSO-$d_6$, ppm) $\delta$ = −4.38 (bs, 3P). $^1$H NMR (400 MHz, $CDCl_3$, ppm) $\delta$ = 8.52 (bs, 3H, $H_{L(Pyr)}$), 7.45−7.41 (m, 18H, $H_{L(Pyr)}$, $H_{L(Ph)}$), 7.31−7.27 (m, 6H, $H_{L(Ph)}$), 7.21−7.17 (m, 12H, $H_{L(Ph)}$), 7.12−7.08 (m, 3H, $H_{L(Pyr)}$). $^{13}$C NMR (101 MHz, $CDCl_3$, ppm) $\delta$ = 160.0 (d, $J_{CP}$ = 35.1 Hz, 3C, $C_{qL(Pyr)}$), 150.4 (d, $J_{CP}$ = 12.7 Hz, 3C, $C_{L(Pyr)}$), 135.8 (d, $J_{CP}$ = 6.2 Hz, 3C, $C_{L(Pyr)}$), 134.4 (d, $J_{CP}$ = 15.5 Hz, 12C, $C_{L(Ph)}$), 133.7 (d, $J_{CP}$ = 19.0 Hz, 6C, $C_{qL(Ph)}$), 129.8 (d, $J_{CP}$ = 23.0 Hz, 3C, $C_{L(Pyr)}$), 129.5 (s, 6C, $C_{L(Ph)}$), 128.5 (d, $J_{CP}$ = 8.6 Hz, 12C, $C_{L(Ph)}$), 123.1 (s, 3C, $C_{L(Pyr)}$). $^{31}$P{$^1$H} NMR (162 MHz, $CDCl_3$, ppm) $\delta$ = −3.20 (s, 3P). MS (FAB, 3-NBA) *m*/*z* [%] = 950 (3) $[M + Cu]^+$, 852 (9) $[M - Cl]^+$, 687 (7) $[Cu_2ClL_2]^+$, 589 (83) $[CuL_2]$, 460 (5) [3-NBA], 423 (5) $[Cu_2ClL]^+$, 326 (52) $[CuL]^+$, 307 (37) [3-NBA], 264 (40) $[L + H]^+$, 185 (13) $[PPh_2]^+$, 154 (100) [3-NBA], 137 (63) [3-NBA]. IR (ATR) $\tilde{\nu}$ [cm$^{-1}$] = 3043 (vw), 1571 (w), 1481 (w), 1448 (w),1433 (m), 1419 (w), 1185 (vw), 1153 (vw), 1093 (w), 1047 (vw), 1027 (vw), 987 (w), 766 (w), 740 (m), 692 (m), 618 (w), 505 (m), 444 (w), 409 (w). Anal. calcd for $C_{51}H_{42}ClCuN_3P_3$ (%): C, 68.92; H, 4.76; N, 4.73. Found: C, 67.73; H, 4.71; N, 4.72. mp = 172 °C.

*2.2.2. CuBrL$_3$.* Yield: 0.975 g (83%). $^1$H NMR (400 MHz, DMSO-$d_6$, ppm) $\delta$ = 8.49 (d, $J_{HH}$ = 4.3 Hz, 3H, $H_{L(Pyr)}$), 7.60 (tt, $J_{HH}$ = 7.7 Hz, $J_{HH}$ = 2.3 Hz, 3H, $H_{L(Pyr)}$), 7.38−7.24 (m, 36H, $H_{L(Pyr)}$, $H_{L(Ph)}$). $^{31}$P{$^1$H} NMR (162 MHz, DMSO-$d_6$, ppm) $\delta$ = −4.60 (bs, 3P). $^{13}$C NMR (101 MHz, DMSO-$d_6$, ppm) $\delta$ = 159.9 (d, $J_{CP}$ = 28.3 Hz, 3C, $C_{qL(Pyr)}$), 149.9 (d, $J_{CP}$ = 12.4 Hz, 3C, $C_{L(Pyr)}$), 135.9 (d, $J_{CP}$ = 5.7 Hz, 3C, $C_{L(Pyr)}$), 134.0 (d, $J_{CP}$ = 11.9 Hz, 6C, $C_{qL(Ph)}$), 133.9 (d, $J_{CP}$ = 16.1 Hz, 12C, $C_{L(Ph)}$), 129.4 (s, 6C, $C_{L(Ph)}$), 128.7 (d, $J_{CP}$ = 22.7 Hz, 3C, $C_{L(Pyr)}$), 128.3 (d, $J_{CP}$ = 8.2 Hz, 12C, $C_{L(Ph)}$), 123.2 (bs, 3C, $C_{L(Pyr)}$). MS (FAB, 3-NBA) *m*/*z* [%] = 994 (1) $[M + Cu]^+$, 852 (1) $[M - Br]^+$, 730 (2) $[Cu_2BrL_2]^+$, 589 (15) $[CuL_2]$, 460 (7) [3-NBA], 326 (10) $[CuL]^+$, 307 (37) $[3\text{-NBA}]^+$, 264 (9) $[L + H]^+$, 185 (3) $[PPh_2]^+$, 154 (100) [3-NBA], 137 (77) [3-NBA]. IR (ATR) $\tilde{\nu}$ [cm$^{-1}$] = 3043 (vw), 1571 (w), 1481 (w), 1449 (w),1433 (w), 1418 (w), 1184 (vw), 1152 (vw), 1092 (w), 1048 (vw), 1027 (vw), 987 (w), 766 (w), 741 (m), 694 (m), 619 (vw), 506 (m), 488 (m), 440 (w), 412 (w). Anal. calcd for $C_{51}H_{42}BrCuN_3P_3$: C 65.63, H 4.54, N 4.50; found: C 63.07, H 4.37, N 4.47. mp = 207 °C.

**2.3. General Procedure for the Synthesis of [AgX(PyrPhos)$_3$] (AgXL$_3$, X = Cl, Br, I) Complexes.** PyrPhos (1.00 g, 3.80 mmol, 3.00 equiv) and AgX (0.181 g for AgCl, 0.238 g for AgBr, 0.297 g for AgI, 1.26 mmol, 1.00 equiv) were suspended in 15 mL of acetonitrile. The reaction mixture was degassed with Ar for 5 min and stirred for 24 h at 90 °C. The suspension consisted of a clear solution and a white solid. The solid was filtered off, washed with acetonitrile (2 × 25 mL), and dried *in vacuo* in the dark. The complexes were obtained as colorless powders and crystallized from hot ethanol ($\mathbf{AgClL_3}$), deuterated DMSO ($\mathbf{AgBrL_3}$), and the acetonitrile filtrate in the freezer ($\mathbf{AgIL_3}$).

*2.3.1. AgClL$_3$.* Yield: 1.03 g (88%). $^1$H NMR (400 MHz, DMSO-$d_6$, ppm) $\delta$ = 8.52 (d, $J_{HH}$ = 4.6 Hz, 3H, $H_{L(Pyr)}$), 7.65 (tdd, $J_{HH}$ = 7.8 Hz, $J_{HH}$ = 2.9 Hz, $J_{HH}$ = 1.8 Hz, 3H, $H_{L(Pyr)}$), 7.43−7.26 (m, 36H, $H_{L(Pyr)}$, $H_{L(Ph)}$). $^{31}$P{$^1$H} NMR (162 MHz, DMSO-$d_6$, ppm) $\delta$ = 3.31 (s, 3P). $^{13}$C NMR (101 MHz, DMSO-$d_6$, ppm) $\delta$ = 159.0 (d, $J_{CP}$ = 31.8 Hz, 3C, $C_{qL(Pyr)}$), 150.3 (d, $J_{CP}$ = 12.8 Hz, 3C, $C_{L(Pyr)}$), 136.2 (d, $J_{CP}$ = 6.7 Hz, 3C, $C_{L(Pyr)}$), 134.0 (d, $J_{CP}$ = 17.2 Hz, 12C, $C_{L(Ph)}$), 133.0 (d, $J_{CP}$ = 14.4 Hz, 6C, $C_{qL(Ph)}$), 129.9 (s, 6C, $C_{L(Ph)}$), 128.9 (d, $J_{CP}$ = 25.8 Hz, 3C, $C_{L(Pyr)}$), 128.6 (d, $J_{CP}$ = 8.8 Hz, 12C, $C_{L(Ph)}$), 123.6 (s, 3C, $C_{L(Pyr)}$). MS (FAB, 3-NBA) *m*/*z* [%] = 1038 (1) $[M + Ag]^+$, 896 (1) $[M - Cl]^+$, 774 (5) $[Ag_2ClL_2]^+$, 633 (65) $[AgL_2]^+$, 370 (100) $[AgL]^+$, 264 (10) $[L + H]^+$, 185 (24)


https://doi.org/10.1021/acsomega.3c05755
ACS Omega 2024, 9, 2220−2233

$[PPh_2]^+$. IR (ATR) $\tilde{\nu}$ [$cm^{-1}$] = 3040 (vw), 1569 (w), 1478 (w), 1448 (w), 1432 (w), 1417 (w), 1183 (vw), 1151 (vw), 1092 (w), 1046 (vw), 1028 (w), 986 (w), 769 (w), 742 (m), 691 (m), 617 (w), 512 (m), 487 (m), 441 (w). Anal. calcd for $C_{51}H_{42}AgClN_3P_3$ (%): C, 65.64; H, 4.54; N, 4.50. Found: C, 65.50; H, 4.51; N, 4.65. mp = 167 °C.

*2.3.2. $AgBrL_3$.* Yield: 0.86 g (70%). $^1$H NMR (400 MHz, DMSO-$d_6$, ppm) $\delta$ = 8.52 (d, $J_{HH}$ = 4.0 Hz, 3H, $H_{L(Pyr)}$), 7.65 (tt, $J_{HH}$ = 7.7 Hz, $J_{HH}$ = 2.3 Hz, 3H, $H_{L(Pyr)}$), 7.41−7.27 (m, 36H, $H_{L(Pyr)}$, $HL_{(Ph)}$). $^{31}P\{^1H\}$ NMR (162 MHz, DMSO-$d_6$, ppm) $\delta$ = 1.81 (s, 3P). $^{13}$C NMR (101 MHz, DMSO-$d_6$, ppm) $\delta$ = 159.4 (d, $J_{CP}$ = 29.0 Hz, 3C, $C_{qL(Pyr)}$), 150.2 (d, $J_{CP}$ = 12.8 Hz, 3C, $C_{L(Pyr)}$), 136.2 (d, $J_{CP}$ = 6.2 Hz, 3C, $C_{L(Pyr)}$), 133.9 (d, $J_{CP}$ = 17.3 Hz, 12C, $C_{L(Ph)}$), 133.3 (d, $J_{CP}$ = 11.7 Hz, 6C, $C_{qL(Ph)}$), 129.8 (s, 6C, $C_{L(Ph)}$), 128.8 (d, $J_{CP}$ = 24.8 Hz, 3C, $C_{L(Pyr)}$), 128.6 (d, $J_{CP}$ = 8.6 Hz, 12C, $C_{L(Ph)}$), 123.5 (s, 3C, $C_{L(Pyr)}$). MS (FAB, 3-NBA) $m/z$ [%] = 869 (1) $[M - Br]^+$, 818 (2) $[Ag_2BrL_2]^+$, 633 (69) $[AgL_2]^+$, 555 (2) $[Ag_2BrL]^+$, 369 (100) $[AgL]^+$, 264 (12) $[L + H]^+$, 185 (29) $[PPh_2]^+$. IR (ATR) $\tilde{\nu}$ [$cm^{-1}$] = 3043 (vw), 1570 (w), 1480 (w), 1448 (w), 1434 (m), 1418 (w), 1150 (w), 1093 (w), 1026 (w), 986 (w), 741 (m), 692 (m), 619 (w), 503 (m), 429 (w). Anal. calcd for $C_{51}H_{42}AgBrN_3P_3$ (%): C, 62.66; H, 4.33; N, 4.30. Found: C, 60.81; H, 4.07; N, 4.19. mp = 162 °C.

*2.3.3. $AgIL_3$.* Yield: 0.63 g (49%). $^1$H NMR (400 MHz, DMSO-$d_6$, ppm) $\delta$ = 8.57 (d, $J_{HH}$ = 4.7 Hz, 3H, $H_{L(Pyr)}$), 7.68 (tdd, $J_{HH}$ = 7.7 Hz, $J_{HH}$ = 2.7 Hz, $J_{HH}$ = 1.8 Hz, 3H, $H_{L(Pyr)}$), 7.43−7.37 (m, 18H, $H_P$), 7.34−7.28 (m, 18H, $H_{L(Pyr)}$, $H_{L(Ph)}$). $^{31}P\{^1H\}$ NMR (162 MHz, DMSO-$d_6$, ppm) $\delta$ = 0.20 (s, 3P). $^{13}$C NMR (101 MHz, DMSO-$d_6$, ppm) $\delta$ = 159.6 (d, $J_{CP}$ = 27.3 Hz, 3C, $C_{qL(Pyr)}$), 150.3 (d, $J_{CP}$ = 12.8 Hz, 3C, $C_{L(Pyr)}$), 136.3 (d, $J_{CP}$ = 5.7 Hz, 3C, $C_{L(Pyr)}$), 133.9 (d, $J_{CP}$ = 17.5 Hz, 12C, $C_{L(Ph)}$), 133.4 (d, $J_{CP}$ = 9.8 Hz, 6C, $C_{qL(Ph)}$), 129.8 (s, 6C, $C_{L(Ph)}$), 128.7 (d, $J_{CP}$ = 25.5 Hz, 3C, $C_{L(Pyr)}$), 128.6 (d, $J_{CP}$ = 8.4 Hz, 12C, $C_{L(Ph)}$), 123.5 (s, 3C, $C_{L(Pyr)}$). MS (FAB, 3-NBA) $m/z$ [%] = 1129 (2) $[M + Ag]^+$, 1024 (1) $[M + H]^+$, 896 (4) $[M - I]^+$, 866 (4) $[Ag_2IL_2]^+$, 633 (86) $[AgL_2]^+$, 460 (5) [3-NBA], 369 (47) $[AgL]^+$, 307 (32) [3-NBA], 264 (100) $[L + H]^+$, 154 (92) [3-NBA], 137 (60) [3-NBA]. IR (ATR) $\tilde{\nu}$ [$cm^{-1}$] = 3042 (vw), 1570 (w), 1480 (w), 1447 (w), 1433 (w), 1417 (w), 1149 (w), 1092 (w), 1046 (vw), 1026 (w), 986 (w), 741 (m), 691 (m), 618 (w), 513 (m), 502 (m), 428 (w), 407 (w). Anal. calcd for $C_{51}H_{42}AgIN_3P_3$ (%): C, 59.78; H, 4.13; N, 4.10. Found: C, 58.13; H, 3.99; N, 4.04. mp = 185 °C.

**2.4. General Procedure for the Synthesis of $[Ag_2X_2(PyrPhos)_3]$ ($Ag_2X_2L_3$, X = Cl, Br) Complexes.** PyrPhos (1.00 g, 3.80 mmol, 3.00 equiv) and AgX (0.363 g for AgCl and 0.475 g for AgBr, 2.53 mmol, 2.00 equiv) were suspended in 15 mL of acetonitrile. The reaction mixture was degassed with Ar for 5 min and was stirred for 24 h at 25 °C. The suspension consisted of a colorless and clear solution and a colorless solid. The solid was filtered off, washed with acetonitrile (2 × 20 mL), and dried *in vacuo* in the dark. The complexes were obtained as colorless powders and crystallized from the acetonitrile filtrate in the freezer.

*2.4.1. $Ag_2Cl_2L_3$.* Yield: 1.15 g (85%). $^1$H NMR (400 MHz, DMSO-$d_6$, ppm) $\delta$ = 8.63 (d, $J_{HH}$ = 4.2 Hz, 3H, $H_{L(Pyr)}$), 7.73 (tdd, $J_{HH}$ = 7.7 Hz, $J_{HH}$ = 3.2 Hz, $J_{HH}$ = 1.8 Hz, 3H, $H_{L(Pyr)}$), 7.57−7.51 (m, 15H, $H_{L(Pyr)}$, $H_{L(Ph)}$), 7.46−7.42 (m, 6H, $H_{L(Ph)}$), 7.40−7.33 (m, 15H, $H_{L(Pyr)}$, $H_{L(Ph)}$). $^{31}P\{^1H\}$ NMR (162 MHz, DMSO-$d_6$, ppm) $\delta$ = 7.30 (s, 3P). $^{13}$C NMR (101 MHz, DMSO-$d_6$, ppm) $\delta$ = 157.4 (d, $J_{CP}$ = 43.5 Hz, 3C, $C_{qL(Pyr)}$), 150.6 (d, $J_{CP}$ = 13.3 Hz, 3C, $C_{L(Pyr)}$), 136.6 (d, $J_{CP}$ = 8.2 Hz, 3C, $C_{L(Pyr)}$), 134.1 (d, $J_{CP}$ = 16.6 Hz, 12C, $C_{L(Ph)}$), 131.7 (d, $J_{CP}$ = 25.1 Hz, 6C, $C_{qL(Ph)}$), 130.4 (s, 6C, $C_{L(Ph)}$), 129.5 (d, $J_{CP}$ = 28.8 Hz, 3C, $C_{L(Pyr)}$), 128.7 (d, $J_{CP}$ = 9.7 Hz, 12C, $C_{L(Ph)}$), 124.2 (s, 3C, $C_{L(Pyr)}$). MS (FAB, 3-NBA) $m/z$ [%] = 1179 (1) $[M + Ag]^+$, 1038 (3) $[M - Cl]^+$, 916 (2) $[Ag_3Cl_2L_2]^+$, 774 (18) $[Ag_2ClL_2]^+$, 653 (2) $[Ag_3Cl_2L]^+$, 633 (72) $[AgL_2]^+$, 511 (4) $[Ag_2ClL]^+$, 369 (100) $[AgL]^+$, 307 (13) [3-NBA], 264 (15) $[L + H]^+$, 185 (20) $[PPh_2]^+$, 154 (49) [3-NBA], 137 (33) [3-NBA]. IR (ATR) $\tilde{\nu}$ [$cm^{-1}$] = 1569 (w), 1479 (w), 1452 (w), 1434 (w), 1419 (w), 1093 (w), 986 (w), 742 (m), 721 (w), 692 (m), 618 (vw), 501 (m), 488 (m), 416 (w). Anal. calcd for $C_{51}H_{42}Ag_2Cl_2N_3P_3$ (%): C, 56.90; H, 3.93; N, 3.90. Found: C, 56.99; H, 3.90; N, 3.95. mp = 164 °C.

*2.4.2. $Ag_2Br_2L_3$.* Yield: 1.06 g (93%). $^1$H NMR (400 MHz, DMSO-$d_6$, ppm) $\delta$ = 8.63 (d, $J_{HH}$ = 4.7 Hz, 3H, $H_{L(Pyr)}$), 7.75 (tdd, $J_{HH}$ = 7.6 Hz, $J_{HH}$ = 3.0 Hz, $J_{HH}$ = 1.8 Hz, 3H, $H_{L(Pyr)}$), 7.51−7.43 (m, 21H, $H_{L(Pyr)}$, $H_{L(Ph)}$), 7.41−7.35 (m, 15H, $H_{L(Pyr)}$, $H_{L(Ph)}$). $^{31}P\{^1H\}$ NMR (162 MHz, DMSO-$d_6$, ppm) $\delta$ = 4.92 (bs, 3P). $^{13}$C NMR (101 MHz, DMSO-$d_6$, ppm) $\delta$ = 158.2 (d, $J_{CP}$ = 37.8 Hz, 3C, $C_{qL(Pyr)}$), 150.6 (d, $J_{CP}$ = 13.3 Hz, 3C, $C_{L(Pyr)}$), 136.5 (d, $J_{CP}$ = 7.1 Hz, 3C, $C_{L(Pyr)}$), 134.0 (d, $J_{CP}$ = 17.0 Hz, 12C, $C_{L(Ph)}$), 132.3 (d, $J_{CP}$ = 19.5 Hz, 6C, $C_{qL(Ph)}$), 130.3 (s, 6C, $C_{L(Ph)}$), 129.1 (d, $J_{CP}$ = 26.6 Hz, 3C, $C_{L(Pyr)}$), 128.8 (d, $J_{CP}$ = 9.2 Hz, 12C, $C_{L(Ph)}$), 124.0 (s, 3C, $C_{L(Pyr)}$). $^1$H NMR (400 MHz, $CDCl_3$, ppm) $\delta$ = 8.62 (d, $J_{HH}$ = 4.7 Hz, 3H, $H_{L(Pyr)}$), 7.81 (t, $J_{HH}$ = 6.9 Hz, 3H, $H_{L(Pyr)}$), 7.63−7.59 (m, 12H, $H_{L(Ph)}$), 7.55 (tdd, $J_{HH}$ = 7.7 Hz, $J_{HH}$ = 3.1 Hz, $J_{HH}$ = 1.8 Hz, 3H, $H_{L(Pyr)}$), 7.38−7.34 (m, 6H, $H_{L(Ph)}$), 7.31−7.27 (m, 12H, $H_{L(Ph)}$), 7.21−7.17 (m, 3H, $H_{L(Pyr)}$). Please note that the reference resonance of $CHCl_3$ could not be picked due to an overlap with the resonances of the compound. $^{31}P\{^1H\}$ NMR (162 MHz, $CDCl_3$, ppm) $\delta$ = 5.94 (s, 3P). $^{13}$C NMR (101 MHz, $CDCl_3$, ppm) $\delta$ = 158.9 (d, $J_{CP}$ = 36.9 Hz, 3C, $C_{qL(Pyr)}$), 150.6 (d, $J_{CP}$ = 12.8 Hz, 3C, $C_{L(Pyr)}$), 136.2 (d, $J_{CP}$ = 8.0 Hz, 3C, $C_{L(Pyr)}$), 134.5 (d, $J_{CP}$ = 16.8 Hz, 12C, $C_{L(Ph)}$), 132.5 (d, $J_{CP}$ = 20.9 Hz, 6C, $C_{qL(Ph)}$), 130.3 (d, $J_{CP}$ = 30.0 Hz, 3C, $C_{L(Pyr)}$), 130.1 (s, 6C, $C_{L(Ph)}$), 128.8 (d, $J_{CP}$ = 9.4 Hz, 12C, $C_{L(Ph)}$), 123.6 (s, 3C, $C_{L(Pyr)}$). MS (FAB, 3-NBA) $m/z$ [%] = 1081 (7) $[M - Br]^+$, 1004 (3) $[Ag_3Br_2L_2]^+$, 896 (23) $[AgL_3]^+$, 822 (100), 818 (37) $[Ag_2BrL_2]^+$. IR (ATR) $\tilde{\nu}$ [$cm^{-1}$] = 3044 (vw), 1569 (w), 1452 (w), 1434 (w), 1418 (w), 1314 (vw), 1182 (vw), 1158 (vw), 1093 (w), 1050 (vw), 1027 (vw), 886 (w), 767 (w), 742 (m), 721 (w), 691 (s), 618 (vw), 501 (s), 488 (m), 431 (w), 416 (w), 395 (w). Anal. calcd for $C_{51}H_{42}Ag_2Br_2N_3P_3$ (%): C, 52.56; H, 3.63; N, 3.61. Found: C, 52.27; H, 3.53; N, 3.58. mp = 184 °C.

**2.5. General Procedure for the Synthesis of $[Ag_4X_4(PyrPhos)_4]$ ($Ag_4X_4L_4$, X = Cl, Br, I) Complexes.** PyrPhos (1.00 g, 3.80 mmol, 4.00 equiv) and AgX (0.544 g, 3.80 mmol, 4.00 equiv) were suspended in 15 mL of acetonitrile. The reaction mixture was degassed with Ar for 5 min and stirred for 24 h at 90 °C. The suspension consisted of a clear solution and a white solid. The solid was filtered off hot, washed with hot acetonitrile (2 × 25 mL), and dried *in vacuo* in the dark. The complexes were obtained as colorless powders and crystallized from acetonitrile filtrates in the freezer.

*2.5.1. $Ag_4Cl_4L_4$.* Yield: 1.44 g (93%). $^1$H NMR (400 MHz, DMSO-$d_6$, ppm) $\delta$ = 8.75 (d, $J_{HH}$ = 4.7 Hz, 4H, $H_{L(Pyr)}$), 7.84 (tdd, $J_{HH}$ = 7.7 Hz, $J_{HH}$ = 3.2 Hz, $J_{HH}$ = 1.8 Hz, 4H, $H_{L(Pyr)}$), 7.59−7.41 (m, 48H, $H_{L(Pyr)}$, $H_{L(Ph)}$). $^{31}P\{^1H\}$ NMR (162 MHz, DMSO-$d_6$, ppm) $\delta$ = 10.24 (s, 4P). $^{13}$C NMR (101 MHz, DMSO-$d_6$, ppm) $\delta$ = 156.7 (d, $J_{CP}$ = 49.3 Hz, 4C, $C_{qL(Pyr)}$), 150.9 (d, $J_{CP}$ = 13.9 Hz, 4C, $C_{L(Pyr)}$), 137.0 (d, $J_{CP}$ =


https://doi.org/10.1021/acsomega.3c05755
ACS Omega 2024, 9, 2220−2233

8.3 Hz, 4C, $C_{L(Pyr)}$), 134.1 (d, $J_{CP}$ = 16.8 Hz, 16C, $C_{L(Ph)}$), 131.0 (d, $J_{CP}$ = 29.7 Hz, 8C, $C_{qL(Ph)}$), 130.8 (d, $J_{CP}$ = 1.9 Hz, 8C, $C_{L(Ph)}$), 129.6 (d, $J_{CP}$ = 28.6 Hz, 4C, $C_{L(Pyr)}$), 129.0 (d, $J_{CP}$ = 10.0 Hz, 16C, $C_{L(Ph)}$), 124.6 (s, 4C, $C_{L(Pyr)}$). $^1$H NMR (400 MHz, $CDCl_3$, ppm) $\delta$ = 8.69 (d, $J_{HH}$ = 4.7 Hz, 4H, $H_{L(Pyr)}$), 7.71−7.68 (m, 4H, $H_{L(Pyr)}$), 7.63−7.60 (m, 4H, $H_{L(Pyr)}$), 7.59−7.54 (m, 16H, $H_{L(Ph)}$), 7.41−7.37 (m, 8H, $H_{L(Ph)}$), 7.34−7.30 (m, 16H, $H_{L(Ph)}$), 7.25−7.21 (m, 4H, $H_{L(Pyr)}$). $^{31}$P{$^1$H} NMR (162 MHz, $CDCl_3$, ppm) $\delta$ = 9.88 (s, 4P). $^{13}$C NMR (101 MHz, $CDCl_3$, ppm) $\delta$ = 157.9 (d, $J_{CP}$ = 160.0 Hz, 4C, $C_{qL(Pyr)}$), 151.0 (d, $J_{CP}$ = 13.5 Hz, 4C, $C_{L(Pyr)}$), 136.4 (d, $J_{CP}$ = 8.5 Hz, 4C, $C_{L(Pyr)}$), 134.5 (d, $J_{CP}$ = 16.5 Hz, 16C, $C_{L(Ph)}$), 131.6 (d, $J_{CP}$ = 108.0 Hz, 8C, $C_{qL(Ph)}$), 130.5 (s, 8C, $C_{L(Ph)}$), 130.4 (d, $J_{CP}$ = 31.3 Hz, 4C, $C_{L(Pyr)}$), 129.0 (d, $J_{CP}$ = 9.9 Hz, 16C, $C_{L(Ph)}$), 124.0 (s, 4C, $C_{L(Pyr)}$). MS (FAB, 3-NBA) $m/z$ [%] = 1726 (1) $[M+Ag]^+$, 1584 (1) $[M - Cl]^+$, 1442 (1) $[Ag_3Cl_2L_4]^+$, 1321 (1) $[Ag_4Cl_3L_3]^+$, 1179 (2) $[Ag_3Cl_2L_3]^+$, 1038 (1) $[Ag_2ClL_3]^+$, 896 (1) $[AgL_3]^+$, 774 (20) $[Ag_2ClL_2]^+$, 633 (63) $[AgL_2]^+$, 511 (4) $[Ag_2ClL]^+$, 460 (7) [3-NBA], 369 (83) $[AgL]^+$, 307 (39) [3-NBA], 264 (24) $[L + H]^+$, 186 (17) $[L - Ph]^+$, 154 (100) [3-NBA], 137 (69) [3-NBA]. IR (ATR) $\tilde{\nu}$ [$cm^{-1}$] = 2163 (vw), 1570 (vw), 1479 (vw), 1449 (vw), 1435 (vw), 1421 (vw), 1278 (vw), 1096 (vw), 1048 (vw), 987 (vw), 775 (vw), 743 (w), 722 (vw), 691 (w), 618 (vw), 515 (w), 502 (w), 438 (vw), 418 (vw), 401 (vw). Anal. calcd for $C_{68}H_{56}Ag_4Cl_4N_4P_4$ (%): C, 50.22; H, 3.47; N, 3.44. Found: C, 49.96; H, 3.40; N, 3.47. mp = 230 °C.

*2.5.2. $Ag_4Br_4L_4$.* Yield: 1.64 g (96%). $^1$H NMR (400 MHz, DMSO-$d_6$, ppm) $\delta$ = 8.73 (d, $J_{HH}$ = 4.8 Hz, 4H, $H_{L(Pyr)}$), 7.85 (tdd, $J_{HH}$ = 7.7 Hz, $J_{HH}$ = 3.1 Hz, $J_{HH}$ = 1.8 Hz, 4H, $H_{L(Pyr)}$), 7.57−7.42 (m, 48H, $H_{L(Pyr)}$, $H_{L(Ph)}$). $^{31}$P{$^1$H} NMR (162 MHz, DMSO-$d_6$, ppm) $\delta$ = 8.88 (bs, 4P). $^1$H NMR (400 MHz, $CDCl_3$, ppm) $\delta$ = 8.63 (d, $J_{HH}$ = 4.7 Hz, 4H, $H_{L(Pyr)}$), 7.66−7.63 (m, 4H, $H_{L(Pyr)}$), 7.59−7.52 (m, 20H, $H_{L(Pyr)}$, $H_{L(Ph)}$), 7.39−7.35 (m, 8H, $H_{L(Ph)}$), 7.32−7.28 (m, 16H, $H_{L(Ph)}$), 7.21−7.18 (m, 4H, $H_{L(Pyr)}$). $^{31}$P{$^1$H} NMR (162 MHz, $CDCl_3$, ppm) $\delta$ = 6.47 (s, 4P). $^{13}$C NMR (101 MHz, $CDCl_3$, ppm) $\delta$ = 158.9 (d, $J_{CP}$ = 62.8 Hz, 4C, $C_{qL(Pyr)}$), 150.8 (d, $J_{CP}$ = 52.0 Hz, 4C, $C_{L(Pyr)}$), 136.2 (d, $J_{CP}$ = 31.6 Hz, 4C, $C_{L(Pyr)}$), 134.5 (d, $J_{CP}$ = 16.8 Hz, 16C, $C_{L(Ph)}$), 132.4 (d, $J_{CP}$ = 85.2 Hz, 8C, $C_{qL(Ph)}$), 130.2 (d, $J_{CP}$ = 100.4 Hz, 4C, $C_{L(Pyr)}$), 130.2 (s, 8C, $C_{L(Ph)}$), 128.9 (d, $J_{CP}$ = 9.5 Hz, 16C, $C_{L(Ph)}$), 123.7 (s, 4C, $C_{L(Pyr)}$). MS (FAB, 3-NBA) $m/z$ [%] = Due to the poor solubility of the complex, no mass spectrum could be recorded. IR (ATR) $\tilde{\nu}$ [$cm^{-1}$] = 1568 (w), 1478 (w), 1446 (w), 1434 (w), 1420 (w), 1275 (vw), 1095 (w), 1028 (vw), 988 (w), 771 (w), 743 (m), 723 (w), 692 (m), 618 (vw), 514 (m), 503 (m), 491 (m), 447 (w), 422 (w). Anal. calcd for $C_{68}H_{56}Ag_4Br_4N_4P_4$ (%): C, 45.27; H, 3.13; N, 3.11. Found: C, 45.32; H, 3.07; N, 3.15. mp = 258 °C.

*2.5.3. $Ag_4I_4L_4$.* Yield: 1.78 g (94%). $^1$H NMR (400 MHz, DMSO-$d_6$, ppm) $\delta$ = 8.71 (d, $J_{HH}$ = 4.6 Hz, 4H, $H_{L(Pyr)}$), 7.82−7.77 (m, 4H, $H_{L(Pyr)}$), 7.51−7.39 (m, 48H, $H_{L(Pyr)}$, $H_{L(Ph)}$). $^{31}$P{$^1$H} NMR (162 MHz, DMSO-$d_6$, ppm) $\delta$ = 2.19 (bs, 4P). $^1$H NMR (400 MHz, $CDCl_3$, ppm) $\delta$ = 8.69 (d, $J_{HH}$ = 4.7 Hz, 4H, $H_{L(Pyr)}$), 7.55−7.50 (m, 24H, $H_{L(Pyr)}$, $H_{L(Ph)}$), 7.39−7.29 (m, 24H, $H_{L(Pyr)}$, $H_{L(Ph)}$), 7.19 (qd, $J_{HH}$ = 4.7 Hz, $J_{HH}$ = 1.7 Hz, 4H, $H_{L(Pyr)}$). $^{31}$P{$^1$H} NMR (162 MHz, $CDCl_3$, ppm) $\delta$ = −0.21 (bs, 4P). $^{13}$C NMR (101 MHz, $CDCl_3$, ppm) $\delta$ = 150.6 (d, $J_{CP}$ = 12.3 Hz, 4C, $C_{L(Pyr)}$), 136.2 (d, $J_{CP}$ = 7.0 Hz, 4C, $C_{L(Pyr)}$), 134.5 (d, $J_{CP}$ = 17.5 Hz, 16C, $C_{L(Ph)}$), 133.7 (d, $J_{CP}$ = 8.9 Hz, 8C, $C_{qL(Ph)}$), 132.3 (d, $J_{CP}$ = 9.6 Hz, 4C, $C_{qL(Pyr)}$), 129.8 (s, 8C, $C_{L(Ph)}$), 128.8 (d, $J_{CP}$ = 8.7 Hz, 16C, $C_{L(Ph)}$), 128.5 (d, $J_{CP}$ = 12.0 Hz, 4C, $C_{L(Pyr)}$), 123.3 (s, 4C, $C_{L(Pyr)}$). MS (FAB, 3-NBA) $m/z$ [%] = Due to the poor solubility of the complex, no mass spectrum could be recorded. IR (ATR) $\tilde{\nu}$ [$cm^{-1}$] = 3043 (vw), 1568 (vw), 1477 (vw), 1446 (w), 1434 (w), 1419 (w), 1276 (vw), 1151 (vw), 1094 (w), 1046 (vw), 1027 (vw), 987 (vw), 844 (vw), 766 (w), 742 (w), 722 (vw), 692 (w), 618 (vw), 511 (w), 501 (w), 422 (w), 395 (vw). Anal. calcd for $C_{68}H_{56}Ag_4I_4N_4P_4$ (%): C, 41.00; H, 2.83; N, 2.81. Found: C, 41.00; H, 2.70; N, 2.85. mp = 272 °C.

**2.6. General Procedure for the Synthesis of Heterobimetallic [MM′$X_2$(PyrPhos)$_3$] (MM′$X_2L_3$, M = Cu, Ag; X = Cl, Br, I) Complexes.** PyrPhos (0.50 g, 1.90 mmol, 3.00 equiv), CuX (0.63 mmol, 1.00 equiv), and AgX (0.63 mmol, 1.00 equiv) were suspended in 15 mL of acetonitrile. The reaction mixture was degassed with Ar for 5 min and stirred for 24 h at 90 °C in the case of **MM′$Cl_2L_3$** and **MM′$Br_2L_3$**, and at 25 °C in the case of **MM′$I_2L_3$**. The light-yellow solids were filtered off hot, washed with acetonitrile (2 × 25 mL), and dried *in vacuo* in the dark. Yields are calculated considering a ratio 1:1 between Ag(I) and Cu(I). The complexes were crystallized from the slow diffusion of *n*-pentane into acetonitrile solutions.

*2.6.1. MM′$Cl_2L_3$.* Yield: 70% (0.45 g). $^1$H NMR (400 MHz, DMSO-$d_6$, ppm) $\delta$ = 8.77 (bs, 3H, $H_{L(Pyr)}$), 7.80 (t, $J_{HH}$ = 7.6 Hz, 3H, $H_{L(Pyr)}$), 7.47−7.34 (m, 36H, $H_{L(Pyr)}$, $H_{L(Ph)}$). $^{31}$P{$^1$H} NMR (162 MHz, DMSO-$d_6$, ppm) $\delta$ = 4.73 (bs, 3P). $^{13}$C NMR (101 MHz, DMSO-$d_6$, ppm) $\delta$ = 157.3 (d, $J_{CP}$ = 47.3 Hz, 3C, $C_{qL(Pyr)}$), 150.8 (d, $J_{CP}$ = 14.0 Hz, 3C, $C_{L(Pyr)}$), 136.9 (d, $J_{CP}$ = 6.1 Hz, 3C, $C_{L(Pyr)}$), 133.9 (d, $J_{CP}$ = 15.9 Hz, 12C, $C_{L(Ph)}$), 131.5 (d, $J_{CP}$ = 28.1 Hz, 6C, $C_{qL(Ph)}$), 130.4 (s, 6C, $C_{L(Ph)}$), 129.7 (d, $J_{CP}$ = 25.4 Hz, 3C, $C_{L(Pyr)}$), 128.8 (d, $J_{CP}$ = 9.5 Hz, 12C, $C_{L(Ph)}$), 124.6 (s, 3C, $C_{L(Pyr)}$). MS (FAB, 3-NBA) $m/z$ [%] = 1091 (2) $[M + Cu]^+$, 994 (4) $[M - Cl]^+$, 774 (7) $[Ag_2ClL_2]^+$, 730 (17) $[AgCuClL_2]^+$, 687 (13) $[Cu_2ClL_2]^+$, 633 (52) $[AgL_2]^+$, 589 (50) $[CuL_2]^+$, 467 (11) $[AgCuClL]^+$, 423 (24) $[Cu_2ClL]^+$, 369 (62) $[AgL]^+$, 326 (100) $[CuL]^+$, 264 (21) $[L+H]^+$, 185 (27) $[PPh_2]^+$. IR (ATR) $\tilde{\nu}$ [$cm^{-1}$] = 3045 (vw), 1277 (vw), 1569 (w), 1479 (w), 1452 (w), 1434 (w), 1419 (w), 1314 (vw), 1181 (vw), 1159 (vw), 1093 (w), 1050 (vw), 1028 (vw), 997 (w), 987 (w), 846 (vw), 767 (w), 742 (m), 721 (w), 692 (m), 618 (w), 501 (m), 489 (m), 436 (w), 417 (w). Anal. calcd for $C_{51}H_{42}AgCl_2CuN_3P_3$ (%): C, 59.35; H, 4.10; N, 4.07. Found: C, 59.13; H, 4.08; N, 4.15.

*2.6.2. MM′$Br_2L_3$.* Yield: 86% (0.61 g). $^1$H NMR (400 MHz, DMSO-$d_6$, ppm) $\delta$ = 8.75 (bs, 3H, $H_{L(Pyr)}$), 7.80 (t, $J_{HH}$ = 7.7 Hz, 3H, $H_{L(Pyr)}$), 7.46−7.34 (m, 36H, $H_{L(Pyr)}$, $H_{L(Ph)}$). $^{31}$P{$^1$H} NMR (162 MHz, DMSO-$d_6$, ppm) $\delta$ = 2.72 (bs, 3P). Due to the poor solubility of the complex, the $^{13}$C NMR spectrum could be recorded. MS (FAB, 3-NBA) $m/z$ [%] = 1038 (3) $[M - Br]^+$, 994 (4) $[BrCu_2L_3]^+$, 818 (2) $[Ag_2BrL_2]^+$, 774 (9) $[AgBrCuL_2]^+$, 730 (19) $[BrCu_2L_2]^+$, 633 (39) $[AgL_2]^+$, 589 (49) $[CuL_2]^+$, 511 (6) $[AgBrCuL]^+$, 467 (14) $[BrCu_2L]^+$, 369 (36) $[AgL]^+$. Due to the poor solubility of the complex, only some bulk signals could be assigned. IR (ATR) $\tilde{\nu}$ [$cm^{-1}$] = 3042 (vw), 1569 (w), 1479 (w), 1452 (w), 1434 (m), 1419 (w), 1314 (vw), 1182 (vw), 1159 (w), 1092 (w), 1027 (vw), 987 (w), 767 (m), 742 (m), 720 (w), 692 (s), 618 (w), 502 (s), 489 (s), 435 (w), 417 (w). Anal. calcd for $C_{51}H_{42}AgBr_2CuN_3P_3$ (%): C, 54.64; H, 3.78; N, 3.75. Found: C, 54.12; H, 3.68; N, 3.79.

*2.6.3. MM′$I_2L_3$.* Yield: 95% (0.73 g). $^1$H NMR (400 MHz, DMSO-$d_6$, ppm) $\delta$ = 8.66 (bs, 3H, $H_{L(Pyr)}$), 7.73 (t, $J_{HH}$ = 6.9 Hz, 3H, $H_{L(Pyr)}$), 7.44−7.31 (m, 36H, $H_{L(Pyr)}$, $H_{L(Ph)}$). $^{31}$P


https://doi.org/10.1021/acsomega.3c05755
ACS Omega 2024, 9, 2220−2233

NMR (162 MHz, DMSO-$d_6$, ppm) $\delta = -1.43$ (bs, 3P). Due to the poor solubility of the complex, the $^{13}$C NMR spectrum could be recorded. MS (FAB, 3-NBA) $m/z$ [%] = 1088 (10) $[M - I]^+$, 1043 (17) $[Cu_2IL_3]^+$, 866 (18) $[Ag_2IL_2]^+$, 780 (40) $[Cu_2IL_2]^+$, 749 (64) $[AgCu_2I_2L]^+$. Due to the poor solubility of the complex, only some bulk signals could be assigned. IR (ATR) $\tilde{\nu}$ [cm$^{-1}$] = 3040 (vw), 1585 (m), 1570 (w), 1479 (w), 1451 (w), 1434 (w), 1418 (w), 1183 (vw), 1157 (w), 1093 (w), 1027 (vw), 988 (w), 765 (w), 742 (m), 720 (w), 692 (m), 618 (vw), 505 (m), 491 (m), 419 (w). Anal. calcd for $C_{51}H_{42}AgCuI_2N_3P_3$ (%): C, 50.41; H, 3.48; N, 3.46. Found: C, 50.91; H, 3.47; N, 3.66.

**2.7. SEM–EDX Measurements.** The approximate metal ratios of the heterobimetallic samples were studied through scanning electron microscopy (SEM) in combination with energy-dispersive X-ray spectroscopy (EDX). The spectra were measured at 20 keV using an Oxford INCA 350 energy-dispersive X-ray spectrometer connected with a Hitachi S-4800 scanning electron microscope (SEM). For the EDX measurements, a small amount of each sample was taken. The powder samples were attached to the SEM specimen stubs using a conductive double-sided carbon adhesive tape and coated with a thin layer of carbon to improve conductivity. Measurements were made from a large area to obtain an average composition and from points to study compositional variations. For compound **MM′Cl$_2$L$_3$** (M/M′ = Cu or Ag), only one sample was investigated, whereas for **MM′Br$_2$L$_3$** and **MIL$_3$** samples, respectively, from five and two different vials were considered (the complete data are collected in the Supporting Information).

**2.8. DFT Calculations.** The Turbomole program package[67] and the resolution-of-the-identity (RI) approximation were used for all calculations. The ground-state structures were optimized using CAM-B3LYP/def2-TZVP (def2-SV(P) for H).[68] For Ag and I, effective core potentials (ECPs) were used. In all of the calculations, an integration grid of size 4 was used. Weight derivatives were used for all optimizations. Convergence criteria for the ground-state structures were set to $10^{-8}$ $E_h$ for the energy and $10^{-6}$ $E_h/a_0$ for the gradient.

## 3. RESULTS AND DISCUSSION

**3.1. Synthesis of the Complexes.** Mononuclear Cu(I) and Ag(I) complexes having general formulas **MXL$_3$** (M = Cu, Ag; X = Cl, Br) were obtained by reacting PyrPhos and the corresponding Cu(I) or Ag(I) halide in ratio 3:1. In the first case, the reaction was carried out at room temperature in dichloromethane, while for Ag(I) derivatives, acetonitrile as solvent and $T$ = 90 °C were required. In the case of **CuBrL$_3$**, **AgBrL$_3$**, and **AgIL$_3$**, the carbon content measured *via* elemental analysis was unexpectedly low, probably due to the hygroscopicity of the complexes. Regarding the dinuclear homometallic PyrPhos Cu(I) complexes, **Cu$_2$X$_2$L$_3$** (with L = PyrPhos, X = Cl, Br, I) were synthesized in dichloromethane at room temperature according to the literature procedure reported by Zink and co-workers.[65] The corresponding Ag(I) derivatives **Ag$_2$X$_2$L$_3$** (with L = PyrPhos, X = Cl, Br) were prepared in acetonitrile at room temperature in dark conditions, as depicted in Scheme 1. The complexes **Ag$_2$Cl$_2$L$_3$** and **Ag$_2$Br$_2$L$_3$** were obtained as colorless powders in contrast to their Cu(I) analogues that are pale yellow-colored. Unfortunately, the iodide analogue **Ag$_2$I$_2$L$_3$** was not accessible using the same reaction conditions described for the chloride and bromide complexes.

**Scheme 1. Synthesis of the Dinuclear Homometallic Ag(I) PyrPhos Complexes AgX$_2$L$_3$ (L = PyrPhos; X = Cl, Br)**

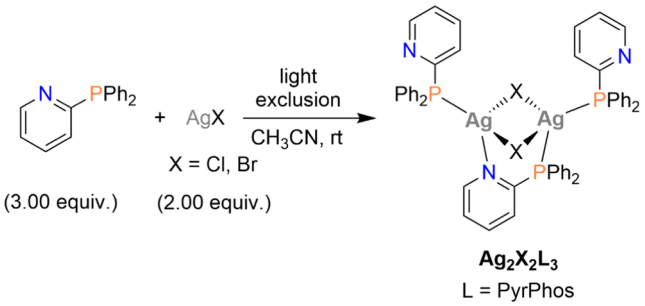


In preliminary experiments, crystals of **Ag$_2$Cl$_2$L$_3$** were obtained from the reaction of the PyrPhos ligand with freshly prepared silver chloride (2:1 ratio) in ethanol after refluxing for 8 h in the dark. **AgClL$_3$** and **Ag$_4$Cl$_4$L$_4$** were obtained as impurities, as suggested by elemental analysis measurements, where ratios, respectively, of 1:1 and 1:3 of PyrPhos and AgCl were detected. The tetranuclear complexes having general formulas **Ag$_4$X$_4$L$_4$** (X = Cl, Br, I) were prepared following the same synthetic procedure employed for **AgXL$_3$** but with a ratio 1:1 between AgX (X = Cl, Br, I) and PyrPhos. Crystals of the dinuclear Ag(I) PyrPhos chloro-complex **Ag$_2$Cl$_2$L$_4$** were isolated as impurities and analyzed by single-crystal X-ray diffraction (*vide infra*). However, the direct synthesis of the **Ag$_2$X$_2$L$_4$** complexes exploiting the reaction conditions used for the synthesis of the other PyrPhos complexes (dichloromethane at rt, $CH_3CN$ at rt, and $CH_3CN$ at 90 °C) was not successful. In general, the formation of the tetranuclear Ag(I) PyrPhos complexes was favored at high temperatures.

The solubility of both Cu(I) and Ag(I) homometallic complexes was investigated in various solvents (see the Supporting Information for details and Table S1 for the complete data). In general, their solubility is relatively low compared to various other homo- and heteroleptic Cu(I) complexes bearing at least one NP-bridging ligand with additional substituents on the pyridine, such as methyl or *tert*-butyl.[52,69] Almost none of the Cu(I) and Ag(I) complexes reported in this study showed a solubility higher than 1 mg mL$^{-1}$ in *n*-hexane, toluene, ethanol, and acetonitrile. In dichloromethane and chlorobenzene, the solubility of the metal complexes increased with the size of the corresponding halide, Cl > Br > I. In addition, the monometallic Cu(I) and Ag(I) complexes **MXL$_3$** are far more soluble in chlorinated solvents compared to the dimetallic complexes **M$_2$X$_2$L$_3$**, while the tetrametallic complexes **M$_4$X$_4$L$_4$** are hardly soluble at all. In general, the solubility of the Cu(I) complexes was similar or higher compared to the corresponding Ag(I) complexes.

With the homometallic Cu(I) and Ag(I) complexes in hand, we deemed it interesting to synthesize heterobimetallic PyrPhos complexes having the general formula **MM′X$_2$L$_3$** (M/M′ = Cu, Ag). It is worth mentioning that the first heterobimetallic Ag(I)/Cu(I) complex was reported by Fackler *et al.* in 1992 using the bidentate 2-mercaptothiazoline as a ligand.[70] However, most of the examples described in the literature are heterobimetallic derivatives with four or more metal centers.[71−79] Only using diphenyl(1-pyridyl)phosphine sulfide as a ligand, a dinuclear Ag(I)/Cu(I) complex was isolated by Olmos and co-workers.[80] The reaction of stoichiometric amounts of the PyrPhos ligand with Cu(I) and Ag(I) halides in a ratio 3:1:1 (dichloromethane, rt) in the


https://doi.org/10.1021/acsomega.3c05755
ACS Omega 2024, 9, 2220−2233

dark resulted in a suspension that consisted of a colorless solid ($Ag_4X_4L_4$) and a yellow solution ($Cu_2X_2L_3$). Therefore, acetonitrile was chosen as the solvent for the synthesis of the heterobimetallic Cu(I)/Ag(I) PyrPhos complexes following the conditions described earlier for the preparation of the Ag(I) derivatives. The reactions were carried out at room temperature for $CuAgI_2L_3$, while $T$ = 90 °C was required for the chloro- and bromo-species (see Scheme 2 for completeness). The elemental analyses are in agreement with the expected CHN values for the heterobimetallic Cu(I)/Ag(I) PyrPhos complexes.

**Scheme 2. Synthesis of the Dinuclear Homobimetallic Cu(I)/Ag(I) PyrPhos Complexes $CuAgX_2L_3$ (L = PyrPhos; X = Cl, Br, I)[a]**

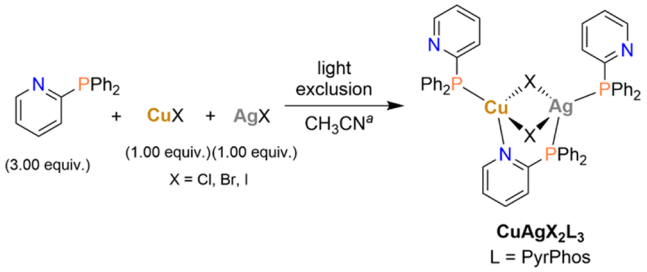


[a] $T$ = 90 °C for $CuAgCl_2L_3$ and $CuAgBr_2L_3$; rt for $CuAgI_2L_3$.

**3.2. Molecular Structure Determination.** The PyrPhos complexes based on Cu(I) and Ag(I) were characterized via single-crystal X-ray diffraction (see the Supporting Information for the experimental details). The molecular structures of $CuClL_3$ and $CuBrL_3$, and $AgXL_3$ (L = PyrPhos, X = Cl, Br, I) are reported in Figures S1–S5. In $AgBrL_3$, a positional disorder of one DMSO solvent molecule was observed. Crystallographic and refinement data are collected in Tables S2 and S3. The metal–halide and metal–phosphorus bond lengths and angles of $CuXL_3$ (X = Cl, Br) and $AgXL_3$ (X = Cl, Br, I) are collected in Table S4, together with the data from the previously reported $CuIL_3$ for comparison.[81] Differently from the Cu(I) complexes, the three $AgXL_3$ complexes are isostructural and crystallized in the triclinic $P\bar{1}$ space group. On the other hand, the $CuXL_3$ derivatives crystallize, respectively, in the orthorhombic $P2_12_12_1$ ($CuClL_3$), in the triclinic $P\bar{1}$ ($CuBrL_3$), and in the trigonal $P\bar{3}$ ($CuIL_3$) space groups.[81]

The structure of the two dinuclear monometallic Ag(I) PyrPhos complexes $Ag_2Cl_2L_3$ and $Ag_2Br_2L_3$ is shown in Figure 1 (see Figures S6 and S7 for the ORTEP). The molecular structure of $Ag_2Cl_2L_3$ is a redetermination of BEBGEU at 123 K.[62] All of the positions of the nitrogen atoms of the PyrPhos ligands in the dinuclear Ag(I) complex could be assigned. Crystallographic and refinement data are collected in Table S5 (see Table S6 for selected bond lengths and angles). Similarly to the corresponding Cu(I) complexes, the two Ag(I) complexes are isostructural and crystallize in the monoclinic space group $P2_1/n$. The Ag(I) derivatives exhibit a butterfly-shaped core where the pyridines of the ancillary PyrPhos ligands coordinate only via the phosphorus atom to the metal, pointing all in the same direction. In contrast, both pyridines of the ancillary PyrPhos ligands are pointing in opposite directions of the bridging PyrPhos ligand in the previously reported $Cu_2I_2L_3$.[65] The bond lengths (Å) of the molecular structures of the dinuclear monometallic PyrPhos complexes $Cu_2X_2L_3$ and $Ag_2X_2L_3$ (X = Cl, Br) and the values found for the computed structures are collected in Table 1 (see Section 2 for details on the DFT calculations).

Complexes with general formulas $Ag_4X_4L_4$ (X = Cl, Br, I) were crystallized from acetonitrile filtrate solutions at low temperatures (see Figure 2). Crystallographic and refinement data are collected in Table S7 (see Table S8 for selected bond lengths and angles). It is worth mentioning that complex $Ag_4Cl_4L_4$ was previously described by Inoguchi and co-workers, and the molecular structure is a redetermination of BUFLOD at 173 K (see Figure S8 for the ORTEP).[63] All of the positions of the nitrogen atoms of the PyrPhos ligands in the tetranuclear Ag(I) complex were assigned. The three derivatives are not isostructural, and they crystallize in the monoclinic space group $C2/c$ ($Ag_4Cl_4L_4$) and in the trigonal space groups $R3c$:$H$ ($Ag_4Br_4L_4$) and $P31c$ ($Ag_4I_4L_4$). The ORTEP plots of $Ag_4Br_4L_4$ and $Ag_4I_4L_4$ are presented in Figures S9 and S10. As previously observed in the mononuclear $AgXL_3$ complexes, all of the PyrPhos ligands are coordinated via the phosphorus atom to the metal also in the tetranuclear Ag(I) complexes. The silver halide core $Ag_4X_4$ of the tetranuclear PyrPhos complexes has a cubane shape. A similar structural motif, *i.e.*, the $Ag_2Cl_2$-core coordinated to four phosphorus atoms of two bidentate phosphines, was reported by Yersin *et al.* in 2014,[84] and a bromide analogue was described by Osawa and co-workers in 2017.[85] Differently from these examples, no evidence of chairlike structures was observed.[86−88] As previously stated, crystals of the dinuclear Ag(I) PyrPhos chloro-complex $Ag_2Cl_2L_4$ were isolated as impurities and analyzed by single-crystal X-ray diffraction (see Figure S11 for the ORTEP). Crystallographic and refinement

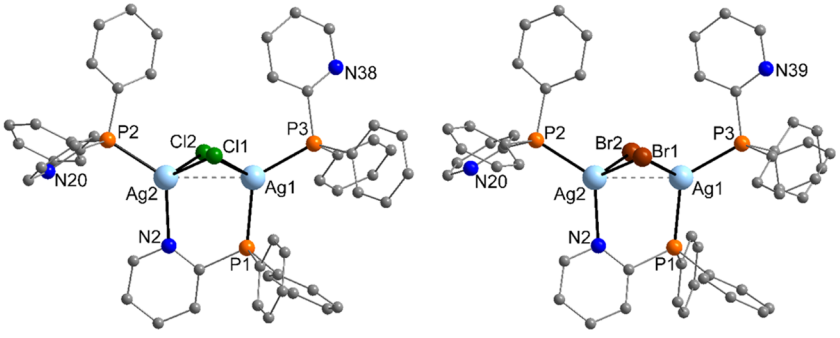


**Figure 1.** Molecular structure of the homometallic Ag(I) PyrPhos complexes $Ag_2Cl_2L_3$ and $Ag_2Br_2L_3$. $Ag_2Cl_2L_3$ is a redetermination of BEBGEU at 123 K.[62] All positions of the nitrogen atoms of the PyrPhos ligands in the dinuclear Ag(I) complex could be assigned.



https://doi.org/10.1021/acsomega.3c05755
ACS Omega 2024, 9, 2220−2233

**Table 1. Overview of the Metal−Metal (M···M) and Metal−Halide (M−X) Bond Lengths in Increasing Order in the Different Homometallic $M_2X_2L_3$ PyrPhos Complexes with M = Cu or Ag and X = Cl or Br (X-ray and Computed Structures) and in the Pure Metal Halides as Starting Materials (Start. Mat.)**

| complex | M···M [Å] X-ray | M−X [Å] X-ray | M···M [Å] computed[a] | M−X [Å] computed[a] | M−X [Å] start. mat.[b] |
|---|---|---|---|---|---|
| $Cu_2Cl_2L_3$[c] | 2.878 | 2.389 | 2.823 | 2.372 | 2.34 |
| | | 2.395 | | 2.414 | |
| | | 2.426 | | 2.443 | |
| | | 2.436 | | 2.461 | |
| average | | 2.412 | | 2.422 | |
| $Cu_2Br_2L_3$[c] | 2.883 | 2.509 | 2.814 | 2.507 | 2.49 |
| | | 2.522 | | 2.554 | |
| | | 2.543 | | 2.575 | |
| | | 2.570 | | 2.587 | |
| average | | 2.536 | | 2.556 | |
| $Ag_2Cl_2L_3$[c] | 3.050 | 2.615 | 3.177 | 2.571 | 2.77 |
| | | 2.620 | | 2.631 | |
| | | 2.652 | | 2.700 | |
| | | 2.688 | | 2.710 | |
| average | | 2.644 | | 2.653 | |
| $Ag_2Br_2L_3$ | 3.030 | 2.722 | 3.138 | 2.692 | 2.89 |
| | | 2.741 | | 2.743 | |
| | | 2.745 | | 2.823 | |
| | | 2.788 | | 2.833 | |
| average | | 2.749 | | 2.773 | |

[a]CAM-B3LYP/def2-TZVP. [b]The values for the metal−halide (M−X) distances of the pure metal halides were taken from the report of Ono and co-workers to complete the data.[82] [c]The data for $Cu_2Cl_2L_3$, $Cu_2Br_2L_3$, and $Ag_2Cl_2L_3$ were obtained from the literature.[62,65,83]

data are collected in Table S9 (see Table S10 for selected bond lengths and angles).

The heterobimetallic Cu(I)/Ag(I) PyrPhos complexes were crystallized from the slow diffusion of *n*-pentane into acetonitrile solutions. Crystallographic and refinement data are collected in Table S11. Structure and geometrical parameters are in the expected range for the $MM'X_2L_3$ derivatives (see Table S12 for selected bond lengths and angles). It is worth mentioning that in the case of the bromo-derivative, two structures with different Cu:Ag ratios were obtained (respectively, 7:1 and 1:7). The molecular structure of the four heterobimetallic complexes is presented in Figure 3 (see also Figures S12−S15). Except for $MM'I_2L_3$ (M/M′ = Cu, Ag), which crystallizes in the triclinic space group $P\bar{1}$, the other three compounds crystallize in the monoclinic space group $P2_1/n$. The heterobimetallic bromo- and chloro-complexes exhibit the same configuration in the PyrPhos ligands as observed in the $MX_2L_3$ complexes (M = Cu, Ag; X = Cl, Br, I). Instead, the equal configuration of the PyrPhos ligands is found in the corresponding heterobimetallic Cu(I)/Ag(I) iodide complex $MM'I_2L_3$.

For the investigation of the heterobimetallic Ag(I)/Cu(I) PyrPhos complexes $MM'X_2L_3$ (M/M′ = Cu, Ag; X = Cl, Br, I), additional scanning electron microscopy with energy-dispersive X-ray analyses (SEM−EDX) was performed to determine the Ag/Cu ratios of the samples (see Section 2 for details). SEM−EDX measurements of PyrPhos complex $MM'Cl_2L_3$ were collected from a large area to obtain an average composition and from points to find out compositional variations. The Cu:Ag molar ratio varies from point to point, being between 0.6:1 and 2:1 (see Table 2). The measurement area and points and the SEM−EDX spectra are shown in Figure 4. In the selected crystal (representative for the sample) used for the single-crystal X-ray diffraction analysis, the Ag/Cu ratio is determined as 1:1. It was deviated from the free refinement of the occupancies of Ag and Cu at position 1 **M**(P/N) and position 2 **M′**(P/P) at the isotropic stage of the refinement and then fixed for the anisotropic refinement (see CIF data for details).

The structure is an $MM'Cl_2L_3$ complex with **M** (position 1) = Cu or Ag and **M′** (position 2) = Cu or Ag. As observable in Table 3, due to the disorder of the Ag(I) and Cu(I) atoms, there are four possible types of bi- and/or monometallic structures for position 1 **M**(P/N) and position 2 **M′**(P/P) (type 1: Ag(P/N)/Cu(P/P); type 2: Cu(P/N)/Ag(P/P); type 3: Ag(P/N)/Ag(P/P); type 4: Cu(P/N)/Cu(P/P)).

The experiments highlight that the monometallic complexation is preferred, with the formation of the $Ag_2Cl_2L_3$ (type 3) or $Cu_2Cl_2L_3$ (type 4) complexes with a maximum occupancy of 40% each. On the other hand, for the heterobimetallic complexes, the formation of type 1 complex $AgCuCl_2L_3$ is favored (minimum occupancy 20%). This is in good correlation with the results found in the two molecular structures of $MM'Br_2L_3$ and in $MM'I_2L_3$ (see Figure 5). In complex $MM'Br_2L_3$ (with a general excess of Cu), the occupancy at position 1 was found as Ag/Cu 15:85 and at position 2 as Ag/Cu 10:90. In complex $MM'Br_2L_3$ (with a general excess of Ag), the occupancy at position 1 was

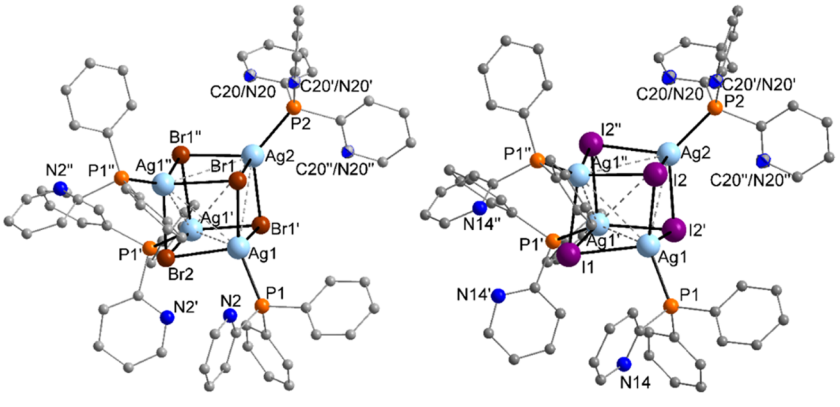


**Figure 2.** Molecular structure of the tetranuclear Ag(I) PyrPhos complexes $Ag_4X_4L_4$ (X = Br, I).



https://doi.org/10.1021/acsomega.3c05755
ACS Omega 2024, 9, 2220−2233

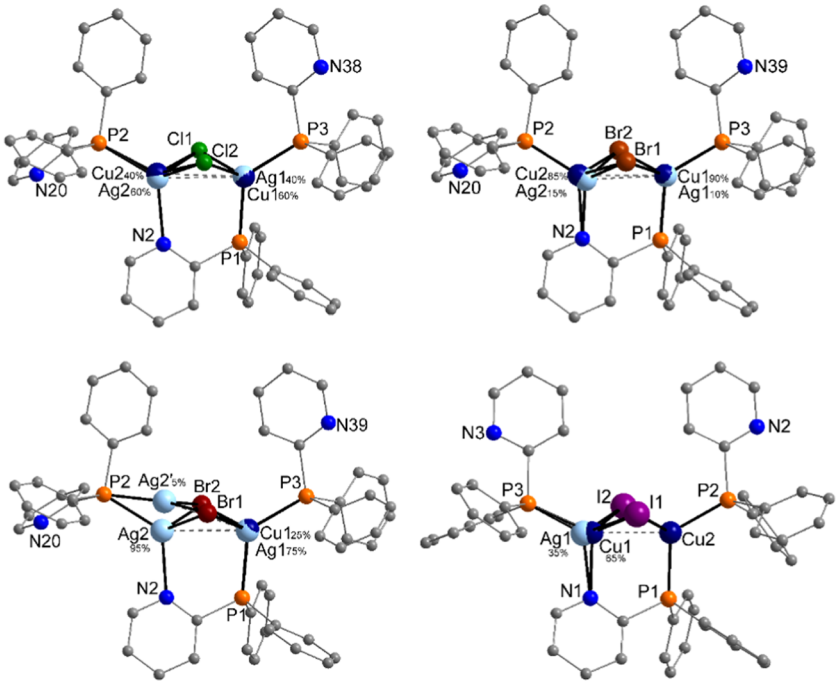


**Figure 3.** Molecular structure of the heterobimetallic Cu(I)/Ag(I) PyrPhos complexes $\mathbf{MM'X_2L_3}$ (M/M′ = Cu, Ag; X = Cl, Br, I). The Cu/Ag ratios are given in percentage.

**Table 2. Element Molar Ratios of the Sample $\mathbf{MM'Cl_2L_3}$ (with M, M′ = Cu or Ag)**[a]

| spectrum | in stats. | C | F | P | Cl | Cu | Ag | Cu/Ag ratio | Cu/Ag ratio[b] |
|---|---|---|---|---|---|---|---|---|---|
| 1 | yes | 91.92 | | 5.01 | 1.63 | 0.99 | 0.46 | 2:1 | |
| 2 | yes | 92.83 | | 3.37 | 2.10 | 0.65 | 1.06 | 0.6:1 | |
| 3 | yes | 86.71 | 1.40 | 5.44 | 3.19 | 1.63 | 1.64 | 1:1 | |
| | | | | | | | | | 0.7:1 |
| max. | | 92.83 | 1.40 | 5.54 | 3.19 | 1.63 | 1.64 | | |
| min. | | 86.71 | 1.40 | 3.37 | 1.63 | 0.65 | 0.46 | | |

[a]All of the elements analyzed are normalized, and all of the results are given in atom %. [b]In large area.

determined as Ag/Ag′ 95:5 and as Ag/Cu 75:25 at position 2. All possible permutations of the complexes $\mathbf{MM'Br_2L_3}$ are presented in Figures S16 and S17 (see Table S15 and Figure S19 for the SEM−EDX measurements conducted on five different vials). In the iodide complex $\mathbf{MM'I_2L_3}$, the occupancy at position 1 was found as Ag:Cu 35:65 (see Figure 3). A type 2 heterobimetallic complex is less probable. This can be justified considering that with the increasing occupancy of the type 2 complex also the occupancy of type 1 is increasing, while the occupancies of type 3 and type 4 complexes are decreasing by the same ratio. In general, the separation of the two bimetallic isomers $\mathbf{AgCuX_2L_3}$ and $\mathbf{CuAgX_2L_3}$ was not possible due to the insolubility of the PyrPhos complexes and the Ag/Cu ratio in the crystals of the PyrPhos complexes was not consistent.

It is worth noting that, in the case of the iodo-derivative, a complex having general formula $\mathbf{MIL_3}$ with M = Cu(I) and Ag(I) in a ratio of 1:1 was isolated as impurity and the structure was investigated through X-ray diffraction (see Figures 5 and S18 for the two possible permutations). Crystallographic and refinement data are collected in Table S13 (see Table S14 for selected bond lengths and angles). The SEM−EDX measurements conducted on two vials containing the $\mathbf{MIL_3}$ complex highlighted a ratio between Ag and Cu of 50:50 (see Figure S20 and Table S16).

**3.3. DFT Calculations.** The singlet ground-state $S_0$ structures of all 12 dinuclear homo- and heterometallic $\mathbf{MM'X_2L_3}$ complexes (M/M′ = Cu, Ag; X = Cl, Br, I) were optimized using CAM-B3LYP/def2-TZVP (def2-SV(P) for hydrogen atoms). To investigate the impact of metal exchange, two starting points for the structure optimizations were chosen (see the Supporting Information for details). The first one (type A) can be described by a synperiplanar conformation with respect to the pyridine groups of the ancillary PyrPhos ligands, which are at the top and almost coplanar. The synperiplanar conformation remained unchanged during the optimization for the homometallic Cu(I) complexes, while a gauche conformation was found for the homometallic Ag(I) complexes, as highlighted in Figure 6a,b. The second starting point (type B) can be described by an anticlinal conformation with respect to the pyridine groups of the ancillary PyrPhos ligands, i.e., with one pyridine ring directed toward the top, while the other one comes out of the plane. This starting point was obtained by a scan of the conformation space; see the Supporting Information for more details. During the optimization, the anticlinal conformation remained unchanged for the homometallic Cu(I) and Ag(I) complexes, as observable for $\mathbf{Cu_2Br_2L_3}$ and $\mathbf{Ag_2Br_2L_3}$ in Figure 6c,d.

Three indicators of structural changes are considered for discussion: the metal−metal (M···M′) distance in addition to



https://doi.org/10.1021/acsomega.3c05755
ACS Omega 2024, 9, 2220−2233

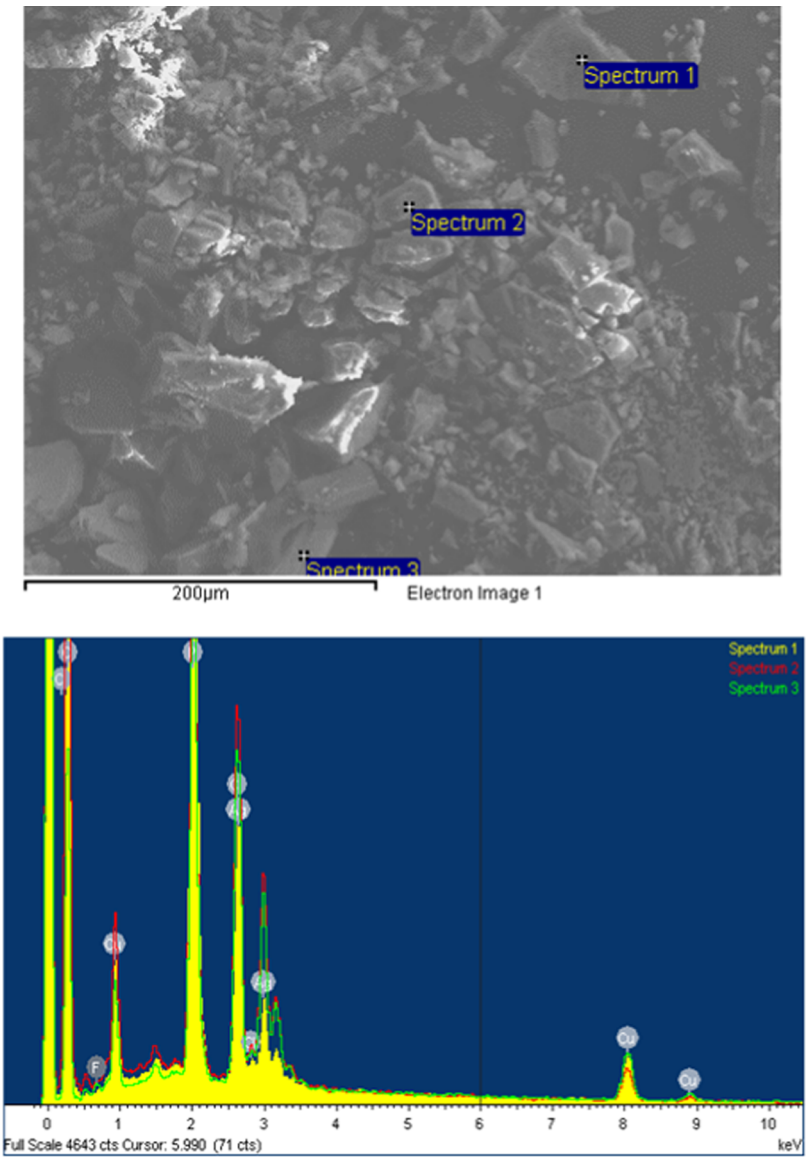


**Figure 4.** Measurement area and points (top) and corresponding SEM−EDX spectra (bottom) of $MM'Cl_2L_3$ complex (M, M′ = Cu or Ag).

**Table 3. Different Possible Types of Bi- and/or Monometallic Structures for Position 1 M(P/N) and Position 2 M′(P/P) in the PyrPhos Complexes $MM'Cl_2L_3$**

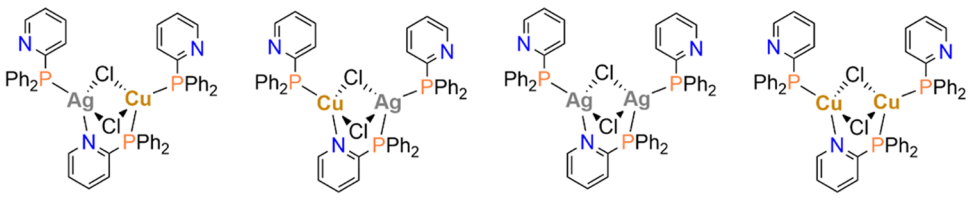


| type | M(P/N) | occupancy M(P/N) [%] | M′(P/P) | occupancy M′(P/P) [%] |
|---|---|---|---|---|
| type 1 | Ag | 20 + $x$ | Cu | 20 + $x$ |
| type 2 | Cu | $x$ | Ag | $x$ |
| type 3 | Ag | 40 − $x$ | Ag | 40 − $x$ |
| type 4 | Cu | 40 − $x$ | Cu | 40 − $x$ |

the distance and Wiberg bond index (WBI) between the metal at M(P/N) and the bridging nitrogen (see Table S17). Overall, the homo- and heterometallic Cu(P/N) complexes are less affected by the conformation of the ancillary PyrPhos ligands compared to the homo- and heterometallic Ag(P/N) complexes. As an example, the results of the bromide complexes as differences of optimized type B structures with respect to optimized type A structures are presented in Table 4



https://doi.org/10.1021/acsomega.3c05755
ACS Omega 2024, 9, 2220−2233

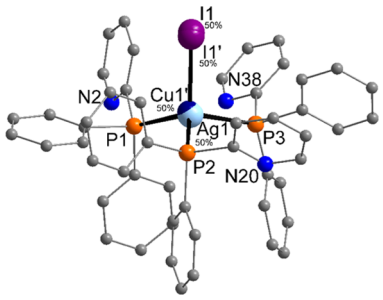


**Figure 5.** Molecular structure of the $MIL_3$ complex (M = Cu, Ag). The Ag/Cu ratios are given in percentage.

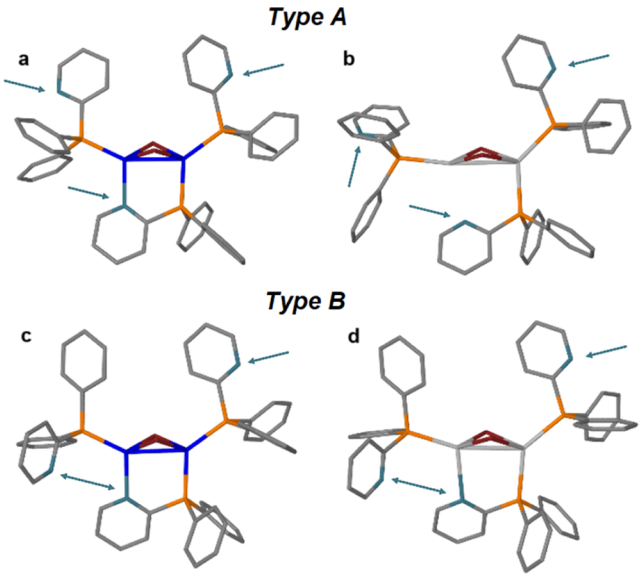


**Figure 6.** Calculated $S_0$ structures of $Cu_2Br_2L_3$ (a, c) and $Ag_2Br_2L_3$ (b, d), starting from synperiplanar conformation (a, b; type A) and anticlinal conformation (c, d; type B). Hydrogen atoms were omitted for clarity (CAM-B3LYP/def2-TZVP; def2-SV(P) for hydrogen atoms). Color map: Cu, blue; Ag, light gray; Br, red; N, sea green (marked with an arrow); P, orange; C, gray. Hydrogen atoms are omitted for clarity.

**Table 4. Difference of the Metal−Metal (M···M′) Distance, Metal−Nitrogen (M−N) Distance, and the Wiberg Bond Index (WBI) between Type B and Type A Structures of the Homo- and Heterometallic Bromide Complexes**

| type B−type A | Δ(M···M′) [Å] | Δ(M−N) [Å] | Δ(WBI) |
|---|---|---|---|
| $Cu_2Br_2L_3$ | −0.003 | −0.021 | +0.03 |
| $CuAgBr_2L_3$ | −0.024 | −0.001 | +0.01 |
| $AgCuBr_2L_3$ | −0.073 | −0.121 | +0.04 |
| $Ag_2Br_2L_3$ | −0.137 | −0.272 | +0.06 |

(see Table S17 for the full data). In the case of $Cu_2Br_2L_3$, the metal−metal (M···M′) and metal−nitrogen (M−N) distances decrease only by 0.003 and 0.021 Å, respectively, from type A (synperiplanar) to type B (anticlinal). The shorter M−N distance is also reflected by the increase of the WBI. A similar trend is observed for $CuAgBr_2L_3$ with Cu(P/N) and Ag(P/P) as the bridging motif is primarily determined by Cu(P/N). Hence, the M−N distance and WBI are less affected than the M···M′ distance, as observable in Tables 4 and S17. Additionally, the M···M′ distance of $CuAgBr_2L_3$ and $AgCuBr_2L_3$ compared to that of $Cu_2Br_2L_3$ is larger by about 0.2 Å. An interesting result was found for $AgCuBr_2L_3$ with Ag(P/N) and Cu(P/P). The M−N distance is increased by about 0.4 Å compared to that of $CuAgBr_2L_3$. This is also reflected in a decrease of WBI from 0.28 to 0.12 passing from type A of $CuAgBr_2L_3$ to $AgCuBr_2L_3$. The trend continues for $Ag_2Br_2L_3$, and a further increase of the M−N distance is observed, leading to a decrease in WBI to 0.06. This weak bridging interaction allows greater flexibility, resulting in a gauche conformation for the pyridine groups of the ancillary PyrPhos ligands in $Ag_2Br_2L_3$ (see Figure 6b). However, for the type B of $Ag_2Br_2L_3$, the anticlinal conformation was found. In this conformation, the M−N distance is reduced by 0.272 Å and the WBI is increased by 0.06 compared to the gauche conformation (type A), indicating a stronger bridging interaction in the anticlinal conformation. This reduces the flexibility, and the ancillary PyrPhos ligands remain in the anticlinal conformation. In addition, as observable in Table S17, the type B structures are also lower in energy by 6.19−7.53 kJ/mol for the homo- and heterometallic Cu(P/N) complexes. Instead, for the homo- and heterometallic Ag(P/N) complexes, this range is decreased to the range −0.51 and 4.76 kJ/mol.

It is worth mentioning that cuprophilic and/or argentophilic interactions were not relevant to the equilibrium structures of the dinuclear complexes presented in this work. Grimme's D3(BJ) dispersion correction for the atom pairs Ag−Ag, Ag−Cu, and Cu−Cu (see Figure S21) and the potential curves clearly show that the metal−metal distances in the X-ray structures are shorter than what would be expected from the dispersion forces. Thus, the metal−metal distances are predominantly determined by the bridging halogen atoms and the ligands.

Furthermore, for all of the homo- and heterometallic Cu(P/N) complexes, the highest occupied molecular orbital (HOMO) and lowest unoccupied molecular orbital (LUMO) are, respectively, located on the metal−halide core and the bridging pyridine group, as shown in Figure 7. In the homo- and heterometallic Ag(P/N) complexes, the LUMO is located at the pyridine group of the PyrPhos ancillary ligand linked to Ag(P/N).

All of the presented data lead to the conclusion that the homo- and heterometallic Cu(P/N) complexes are structurally less affected by the conformation of the ancillary PyrPhos ligands compared to the homo- and heterometallic Ag(P/N) derivatives due to the stronger bridging interaction when Cu(P/N) is present.

## 4. CONCLUSIONS

A series of heteroleptic mono-, di-, and tetranuclear Cu(I) and Ag(I) complexes were synthesized by reacting the corresponding metal−halide with the PyrPhos ligand in different stoichiometries. The molecular structure of almost all of the described complexes was determined by single-crystal X-ray diffraction analysis. However, despite the fact that the molecular structure of $Ag_2Cl_2L_4$ was unambiguously established by X-ray diffraction, the direct synthesis of $Ag_2X_2L_4$ (X = Cl, Br, I; L = PyrPhos) complexes was not favored. In addition, the possible formation of heterobimetallic complexes having the general formula $MM'X_2L_3$ (M/M′ = Cu, Ag; X = Cl, Br, I; L = PyrPhos) was investigated. X-ray diffraction analyses revealed that in the case of $MM'Br_2L_3$ two different structures are possible, with Cu/Ag ratios, respectively, of 7:1 and 1:7. The ratio between the metal centers was studied


https://doi.org/10.1021/acsomega.3c05755
ACS Omega 2024, 9, 2220−2233

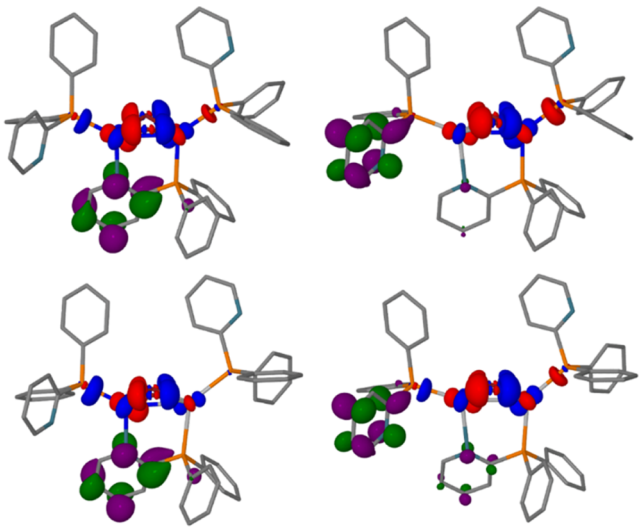

**Figure 7.** HOMO (blue/red) and LUMO (green/purple) of $Cu_2Br_2L_3$ (top left), $AgCuBr_2L_3$ (top right), $CuAgBr_2L_3$ (bottom left), and $Ag_2Br_2L_3$ (bottom right) with anticlinal conformation of the ancillary ligands (CAM-B3LYP/def2-TZVP; def2-SV(P) for hydrogen atoms; isovalue of 0.06 $a_0^{-3/2}$). Color map: Cu, blue; Ag, light gray; Br, red; N, sea green; P, orange; C, gray. Hydrogen atoms are omitted for clarity.

through SEM−EDX measurements for all of the heterobimetallic Cu(I)/Ag(I) complexes. The homo- and heterometallic Ag(I) complexes were compared to their Cu(I) analogues employing DFT calculations, revealing that the latter are less likely to maintain the bridging motive of the PyrPhos ligands if Ag(I) is present. To conclude, the present study extends the use of the PyrPhos ligand to Cu(I) and Ag(I) complexes, as well as to Cu(I)/Ag(I) heterobimetallic species, and it will help the design of the next generation of materials. In particular, the photophysical properties of the latter will be investigated to study the effect of possible cuprophilic and argentophilic interactions, as previously observed for other $d^{10}$ heterobimetallic species.

## ■ ASSOCIATED CONTENT

### Data Availability Statement

The details on the chemical synthesis and original analytical data were added to the repository Chemotion (www.chemotion.net/home). The data are released within the data collection 10.14272/collection/JMB_2020-08-13.[66]

### Supporting Information

The Supporting Information is available free of charge at https://pubs.acs.org/doi/10.1021/acsomega.3c05755.

General information concerning NMR, mass spectrometry, IR, elemental analysis, SEM−EDX and single-crystal X-ray diffraction (XRD) analyses, crystallographic and refinement data, molecular structure and selected bond lengths and angles for the crystallized complexes, and DFT calculations (PDF)

### Accession Codes

CCDC 2063602 ($CuClL_3$,), 2042604 ($Cu_2Br_2L_3$), 2042603 ($AgClL_3$), 2042182 ($AgBrL_3$), 2039548 ($AgIL_3$), 2042183 ($Ag_2Cl_2L_3$), 2039552 ($Ag_2Br_2L_3$), 2039550 ($Ag_2Cl_2L_4$), 2058468 ($Ag_4Cl_4L_4$), 2079569 ($Ag_4Br_4L_4$), 2039549 ($Ag_4I_4L_4$), 2039551 ($CuAgCl_2L_3$), 2062374 ($MIL_3$ with M = Cu or Ag in ratio 1:1), and 2042602 ($CuAgI_2L_3$) contain the supplementary crystallographic data for this paper. These data can be obtained free of charge from The Cambridge Crystallographic Data Centre via www.ccdc.cam.ac.uk/data_request/cif.

## ■ AUTHOR INFORMATION


### Corresponding Authors

**Wim Klopper** − *Institute of Physical Chemistry (IPC) and Institute of Nanotechnology (INT), Karlsruhe Institute of Technology (KIT), 76131 Karlsruhe, Germany;* orcid.org/0000-0002-5219-9328; Email: klopper@kit.edu

**Stefan Bräse** − *Institute of Organic Chemistry (IOC), Karlsruhe Institute of Technology (KIT), 76131 Karlsruhe, Germany; Institute of Biological and Chemical Systems-Functional Molecular Systems (IBCS-FMS), Karlsruhe Institute of Technology (KIT), 76131 Karlsruhe, Germany;* orcid.org/0000-0003-4845-3191; Email: braese@kit.edu

### Authors

**Jasmin M. Busch** − *Institute of Organic Chemistry (IOC), Karlsruhe Institute of Technology (KIT), 76131 Karlsruhe, Germany*

**Florian R. Rehak** − *Institute of Physical Chemistry (IPC), Karlsruhe Institute of Technology (KIT), 76131 Karlsruhe, Germany;* orcid.org/0000-0003-2237-6781

**Valentina Ferraro** − *Institute of Organic Chemistry (IOC), Karlsruhe Institute of Technology (KIT), 76131 Karlsruhe, Germany;* orcid.org/0000-0003-2694-2955

**Martin Nieger** − *Department of Chemistry, University of Helsinki, FI 00014 Helsinki, Finland;* orcid.org/0000-0003-1677-0109

**Marianna Kemell** − *Department of Chemistry, University of Helsinki, FI 00014 Helsinki, Finland;* orcid.org/0000-0002-3583-2064

**Olaf Fuhr** − *Institute of Nanotechnology (INT) and Karlsruhe Nano-Micro Facility (KNMFi), Karlsruhe Institute of Technology (KIT), 76131 Karlsruhe, Germany;* orcid.org/0000-0003-3516-2440

Complete contact information is available at: https://pubs.acs.org/10.1021/acsomega.3c05755


### Author Contributions

The manuscript has been written through the contributions of all authors. J.M.B. and V.F. synthesized and analyzed all presented compounds under the supervision of S.B. The SEM−EDX work was done by M.K., and single-crystal X-ray diffraction analysis was carried out by M.N. and O.F. Theoretical investigations were done by F.R.R. under the supervision of W.K. All authors have approved the final version of the manuscript.

### Notes

The authors declare no competing financial interest.

## ■ ACKNOWLEDGMENTS

The authors dedicate this publication to the memory of their late colleague Markus Gerhards in recognition of his long-standing devotion to the spectroscopic characterization of molecular complexes with and without the involvement of transition-metal centers, which has been pivotal to the present study. The authors are very grateful for the financial support from the Deutsche Forschungsgemeinschaft (DFG) through

the Collaborative Research Center CRC/TRR 88 3MET—Cooperative Effects in Homo- and Heterometallic Complexes (Projects C1, C2 and T1). In addition, the authors wish to thank the Karlsruhe School of Optics and Photonics (KSOP) as well as the DFG for financial support through Germany's Excellence Strategy 3D Matter Made to Order (3DMM2O, Grant No. EXC-2082/1-390761711).

## ■ ABBREVIATIONS

HOMO, highest occupied molecular orbital; LUMO, lowest unoccupied molecular orbital; PyrPhos, 2-(diphenylphosphino)pyridine

## ■ REFERENCES

(1) Yersin, H. *Highly Efficient OLEDs: Materials Based on Thermally Activated Delayed Fluorescence*; Wiley-VCH Verlag, 2019.
(2) Yersin, H.; Rausch, A. F.; Czerwieniec, R.; Hofbeck, T.; Fischer, T. The triplet state of organo-transition metal compounds. Triplet harvesting and singlet harvesting for efficient OLEDs. *Coord. Chem. Rev.* **2011**, *255* (21−22), 2622.
(3) Hong, G.; Gan, X.; Leonhardt, C.; Zhang, Z.; Seibert, J.; Busch, J. M.; Bräse, S. A Brief History of OLEDs—Emitter Development and Industry Milestones. *Adv. Mater.* **2021**, *33* (9), No. 2005630.
(4) Bizzarri, C.; Spuling, E.; Knoll, D. M.; Volz, D.; Bräse, S. Sustainable metal complexes for organic light-emitting diodes (OLEDs). *Coord. Chem. Rev.* **2018**, *373*, 49−82.
(5) Bizzarri, C.; Hundemer, F.; Busch, J. M.; Bräse, S. Triplet emitters versus TADF emitters in OLEDs: A comparative study. *Polyhedron* **2018**, *140*, 51−66.
(6) Uoyama, H.; Goushi, K.; Shizu, K.; Nomura, H.; Adachi, C. Highly efficient organic light-emitting diodes from delayed fluorescence. *Nature* **2012**, *492* (7428), 234−238.
(7) Hosokai, T.; Matsuzaki, H.; Nakanotani, H.; Tokumaru, K.; Tsutsui, T.; Furube, A.; Nasu, K.; Nomura, H.; Yahiro, M.; Adachi, C. Evidence and mechanism of efficient thermally activated delayed fluorescence promoted by delocalized excited states. *Sci. Adv.* **2017**, *3* (5), No. e1603282.
(8) Noda, H.; Nakanotani, H.; Adachi, C. Excited state engineering for efficient reverse intersystem crossing. *Sci. Adv.* **2018**, *4* (6), No. eaao6910.
(9) Muthig, A. M. T.; Mrózek, O.; Ferschke, T.; Rödel, M.; Ewald, B.; Kuhnt, J.; Lenczyk, C.; Pflaum, J.; Steffen, A. Mechano-Stimulus and Environment-Dependent Circularly Polarized TADF in Chiral Copper(I) Complexes and Their Application in OLEDs. *J. Am. Chem. Soc.* **2023**, *145* (8), 4438−4449.
(10) Deaton, J. C.; Switalski, S. C.; Kondakov, D. Y.; Young, R. H.; Pawlik, T. D.; Giesen, D. J.; Harkins, S. B.; Miller, A. J. M.; Mickenberg, S. F.; Peters, J. C. E-Type Delayed Fluorescence of a Phosphine-Supported $Cu_2(\mu\text{-}NAr_2)_2$ Diamond Core: Harvesting Singlet and Triplet Excitons in OLEDs. *J. Am. Chem. Soc.* **2010**, *132* (27), 9499−9508.
(11) Czerwieniec, R.; Yersin, H. Diversity of Copper(I) Complexes Showing Thermally Activated Delayed Fluorescence: Basic Photophysical Analysis. *Inorg. Chem.* **2015**, *54* (9), 4322−4327.
(12) Leitl, M. J.; Zink, D. M.; Schinabeck, A.; Baumann, T.; Volz, D.; Yersin, H. Copper(I) Complexes for Thermally Activated Delayed Fluorescence: From Photophysical to Device Properties. *Top. Curr. Chem.* **2016**, *374*, 141−174.
(13) Ravaro, L. P.; Zanoni, K. P. S.; de Camargo, A. S. S. Luminescent Copper(I) complexes as promising materials for the next generation of energy-saving OLED devices. *Energy Rep.* **2020**, *6*, 37−45.
(14) Hamze, R.; Shi, S.; Kapper, S. C.; Muthiah Ravinson, D. S.; Estergreen, L.; Jung, M.-C.; Tadle, A. C.; Haiges, R.; Djurovich, P. I.; Peltier, J. L.; Jazzar, R.; Bertrand, G.; Bradforth, S. E.; Thompson, M. E. Quick-Silver" from a Systematic Study of Highly Luminescent, Two-Coordinate, $d^{10}$ Coinage Metal Complexes. *J. Am. Chem. Soc.* **2019**, *141* (21), 8616−8626.
(15) Gan, X.-M.; Yu, R.; Chen, X.-L.; Yang, M.; Lin, L.; Wu, X.-Y.; Lu, C.-Z. A unique tetranuclear Ag(i) complex emitting efficient thermally activated delayed fluorescence with a remarkably short decay time. *Dalton Trans.* **2018**, *47* (17), 5956−5960.
(16) Yersin, H.; Czerwieniec, R.; Shafikov, M. Z.; Suleymanova, A. F. TADF Material Design: Photophysical Background and Case Studies Focusing on $Cu^I$ and $Ag^I$ Complexes. *ChemPhysChem* **2017**, *18* (24), 3508−3535.
(17) Klein, M.; Rau, N.; Wende, M.; Sundermeyer, J.; Cheng, G.; Che, C.-M.; Schinabeck, A.; Yersin, H. Cu(I) and Ag(I) Complexes with a New Type of Rigid Tridentate N,P,P-Ligand for Thermally Activated Delayed Fluorescence and OLEDs with High External Quantum Efficiency. *Chem. Mater.* **2020**, *32* (24), 10365−10382.
(18) Tang, M.-C.; Chan, A. K.-W.; Chan, M.-Y.; Yam, V. W.-W. Platinum and gold complexes for OLEDs. *Top. Curr. Chem.* **2016**, *374*, 67−110.
(19) Fernandez-Cestau, J.; Bertrand, B.; Blaya, M.; Jones, G. A.; Penfold, T. J.; Bochmann, M. Synthesis and luminescence modulation of pyrazine-based gold(iii) pincer complexes. *Chem. Commun.* **2015**, *51* (93), 16629−16632.
(20) Li, L.-K.; Tang, M.-C.; Lai, S.-L.; Ng, M.; Kwok, W.-K.; Chan, M.-Y.; Yam, V. W.-W. Strategies towards rational design of gold(iii) complexes for high-performance organic light-emitting devices. *Nat. Photonics* **2019**, *13* (3), 185−191.
(21) Zhou, D.; To, W. P.; Tong, G. S. M.; Cheng, G.; Du, L.; Phillips, D. L.; Che, C. M. Inside Back Cover: Tetradentate Gold(III) Complexes as Thermally Activated Delayed Fluorescence (TADF) Emitters: Microwave-Assisted Synthesis and High-Performance OLEDs with Long Operational Lifetime. *Angew. Chem., Int. Ed.* **2020**, *59* (16), 6631.
(22) Lee, C.-H.; Tang, M.-C.; Kong, F. K.-W.; Cheung, W.-L.; Ng, M.; Chan, M.-Y.; Yam, V. W.-W. Isomeric Tetradentate Ligand-Containing Cyclometalated Gold(III) Complexes. *J. Am. Chem. Soc.* **2020**, *142* (1), 520−529.
(23) Zhou, D.; To, W. P.; Kwak, Y.; Cho, Y.; Cheng, G.; Tong, G. S. M.; Che, C. M. Thermally Stable Donor−Acceptor Type (Alkynyl)-Gold(III) TADF Emitters Achieved EQEs and Luminance of up to 23.4% and 70 300 cd $m^{-2}$ in Vacuum-Deposited OLEDs. *Adv. Sci.* **2019**, *6* (18), No. 1802297.
(24) Mrózek, O.; Mitra, M.; Hupp, B.; Belyaev, A.; Lüdtke, N.; Wagner, D.; Wang, C.; Wenger, O. S.; Marian, C. M.; Steffen, A. An Air- and Moisture-stable Zinc(II) Carbene Dithiolate Dimer Showing Fast Thermally Activated Delayed Fluorescence and Dexter Energy Transfer Catalysis. *Chem. − Eur. J.* **2023**, *29* (23), No. e202203980, DOI: 10.1002/chem.202203980.
(25) Lüdtke, N.; Kuhnt, J.; Heil, T.; Steffen, A.; Marian, C. M. Revisiting Ligand-to-Ligand Charge Transfer Phosphorescence Emission from Zinc(II) Diimine Bis-Thiolate Complexes: It is Actually Thermally Activated Delayed Fluorescence. *ChemPhotoChem* **2023**, *7* (1), No. e202200142, DOI: 10.1002/cptc.202200142.
(26) Sakai, Y.; Sagara, Y.; Nomura, H.; Nakamura, N.; Suzuki, Y.; Miyazaki, H.; Adachi, C. Zinc complexes exhibiting highly efficient thermally activated delayed fluorescence and their application to organic light-emitting diodes. *Chem. Commun.* **2015**, *51* (15), 3181−3184.
(27) Volz, D.; Wallesch, M.; Fléchon, C.; Danz, M.; Verma, A.; Navarro, J. M.; Zink, D. M.; Bräse, S.; Baumann, T. From iridium and platinum to copper and carbon: new avenues for more sustainability in organic light-emitting diodes. *Green Chem.* **2015**, *17* (4), 1988−2011.
(28) Liu, Y.; Li, C.; Ren, Z.; Yan, S.; Bryce, M. R. All-organic thermally activated delayed fluorescence materials for organic light-emitting diodes. *Nat. Rev. Mater.* **2018**, *3*, 18202.
(29) Wong, M. Y.; Zysman-Colman, E. Purely Organic Thermally Activated Delayed Fluorescence Materials for Organic Light-Emitting Diodes. *Adv. Mater.* **2017**, *29* (22), No. 1605444.


https://doi.org/10.1021/acsomega.3c05755
*ACS Omega* 2024, 9, 2220−2233

(30) Zink, D. M.; Bächle, M.; Baumann, T.; Nieger, M.; Kühn, M.; Wang, C.; Klopper, W.; Monkowius, U.; Hofbeck, T.; Yersin, H.; Bräse, S. Synthesis, Structure, and Characterization of Dinuclear Copper(I) Halide Complexes with P∧N Ligands Featuring Exciting Photoluminescence Properties. *Inorg. Chem.* **2013**, *52* (5), 2292−2305.
(31) Hofbeck, T.; Monkowius, U.; Yersin, H. Highly Efficient Luminescence of Cu(I) Compounds: Thermally Activated Delayed Fluorescence Combined with Short-Lived Phosphorescence. *J. Am. Chem. Soc.* **2015**, *137* (1), 399−404.
(32) Wallesch, M.; Volz, D.; Zink, D. M.; Schepers, U.; Nieger, M.; Baumann, T.; Bräse, S. Bright Coppertunities: Multinuclear CuIComplexes with N-P Ligands and Their Applications. *Chem. − Eur. J.* **2014**, *20* (22), 6578−6590.
(33) Paderina, A. V.; Koshevoy, I. O.; Grachova, E. V. Keep it tight: a crucial role of bridging phosphine ligands in the design and optical properties of multinuclear coinage metal complexes. *Dalton Trans.* **2021**, *50* (18), 6003−6033.
(34) Artem'ev, A. V.; Davydova, M. P.; Berezin, A. S.; Ryzhikov, M. R.; Samsonenko, D. G. Dicopper(I) Paddle-Wheel Complexes with Thermally Activated Delayed Fluorescence Adjusted by Ancillary Ligands. *Inorg. Chem.* **2020**, *59* (15), 10699−10706.
(35) Rogovoy, M. I.; Rakhmanova, M. I.; Sukhikh, T. S.; Artem'ev, A. V. Luminescent $[Cu_8I_8L_6]$ wheel and $[Cu_2I_2L_3]$ cage assembled from $Cu^I$ and 3,6-bis(diphenylphosphino)pyridazine. *Mendeleev Commun.* **2021**, *31* (6), 804−806.
(36) Baranov, A. Y.; Berezin, A. S.; Samsonenko, D. G.; Mazur, A. S.; Tolstoy, P. M.; Plyusnin, V. F.; Kolesnikov, I. E.; Artem'ev, A. V. New Cu(I) halide complexes showing TADF combined with room temperature phosphorescence: the balance tuned by halogens. *Dalton Trans.* **2020**, *49* (10), 3155−3163.
(37) Artem'ev, A. V.; Baranov, A. Y.; Rakhmanova, M. I.; Malysheva, S. F.; Samsonenko, D. G. Copper(i) halide polymers derived from tris[2-(pyridin-2-yl)ethyl]phosphine: halogen-tunable colorful luminescence spanning from deep blue to green. *New J. Chem.* **2020**, *44* (17), 6916−6922.
(38) Berezin, A. S.; Artem'ev, A. V.; Komarov, V. Y.; Baranov, A. Y. A copper(i) bromide organic−inorganic zwitterionic coordination compound with a new type of core: structure, luminescence properties, and DFT calculations. *New J. Chem.* **2020**, *44* (23), 9858−9862.
(39) Petrovskii, S. K.; Paderina, A. V.; Sizova, A. A.; Baranov, A. Y.; Artem'Ev, A. A.; Sizov, V. V.; Grachova, E. V. Luminescence behaviour of Au(I)−Cu(I) heterobimetallic coordination polymers based on alkynyl-tris(2-pyridyl)phosphine Au(I) complexes. *Dalton Trans.* **2020**, *49* (38), 13430−13439.
(40) Baranov, A. Y.; Pritchina, E. A.; Berezin, A. S.; Samsonenko, D. G.; Fedin, V. P.; Belogorlova, N. A.; Gritsan, N. P.; Artem'ev, A. V. Beyond Classical Coordination Chemistry: The First Case of a Triply Bridging Phosphine Ligand. *Angew. Chem., Int. Ed.* **2021**, *60* (22), 12577−12584.
(41) Artem'ev, A. V.; Baranov, A. Y.; Berezin, A. S.; Stass, D. V.; Hettstedt, C.; Kuzmina, U. Y. A.; Karaghiosoff, K.; Bagryanskaya, I. Y. TADF and X-ray Radioluminescence of New Cu(I) Halide Complexes: Different Halide Effects on These Processes. *Int. J. Mol. Sci.* **2023**, *24* (6), 5145.
(42) Artem'ev, A. V.; Ryzhikov, M. R.; Taidakov, I. V.; Rakhmanova, M. I.; Varaksina, E. A.; Bagryanskaya, I. Y.; Malysheva, S. F.; Belogorlova, N. A. Bright green-to-yellow emitting Cu(I) complexes based on bis(2-pyridyl)phosphine oxides: synthesis, structure and effective thermally activated-delayed fluorescence. *Dalton Trans.* **2018**, *47* (8), 2701−2710.
(43) Kirst, C.; Zoller, F.; Bräuniger, T.; Mayer, P.; Fattakhova-Rohlfing, D.; Karaghiosoff, K. Investigation of Structural Changes of Cu(I) and Ag(I) Complexes Utilizing a Flexible, Yet Sterically Demanding Multidentate Phosphine Oxide Ligand. *Inorg. Chem.* **2021**, *60* (4), 2437−2445.
(44) Demyanov, Y. V.; Sadykov, E. H.; Rakhmanova, M. I.; Novikov, A. S.; Bagryanskaya, I. Y.; Artem'ev, A. V. Tris(2-Pyridyl)Arsine as a New Platform for Design of Luminescent Cu(I) and Ag(I) Complexes. *Molecules* **2022**, *27* (18), 6059.
(45) Artem'ev, A. V.; Demyanov, Y. V.; Rakhmanova, M. I.; Bagryanskaya, I. Y. Pyridylarsine-based Cu(I) complexes showing TADF mixed with fast phosphorescence: a speeding-up emission rate using arsine ligands. *Dalton Trans.* **2022**, *51* (3), 1048−1055.
(46) Artem'ev, A. V.; Shafikov, M. Z.; Schinabeck, A.; Antonova, O. V.; Berezin, A. S.; Bagryanskaya, I. Y.; Plusnin, P. E.; Yersin, H. Sky-blue thermally activated delayed fluorescence (TADF) based on Ag(i) complexes: strong solvation-induced emission enhancement. *Inorg. Chem. Front.* **2019**, *6* (11), 3168−3176.
(47) Rogovoy, M. I.; Berezin, A. S.; Samsonenko, D. G.; Artem'Ev, A. V. Silver(I)−Organic Frameworks Showing Remarkable Thermo-, Solvato- And Vapochromic Phosphorescence As Well As Reversible Solvent-Driven 3D-to-0D Transformations. *Inorg. Chem.* **2021**, *60* (9), 6680−6687.
(48) Artem'ev, A. V.; Eremina, J. A.; Lider, E. V.; Antonova, O. V.; Vorontsova, E. V.; Bagryanskaya, I. Yu. Luminescent Ag(I) scorpionates based on tris(2-pyridyl)phosphine oxide: Synthesis and cytotoxic activity evaluation. *Polyhedron* **2017**, *138*, 218−224.
(49) Zink, D. M.; Volz, D.; Baumann, T.; Mydlak, M.; Flügge, H.; Friedrichs, J.; Nieger, M.; Bräse, S. Heteroleptic, Dinuclear Copper(I) Complexes for Application in Organic Light-Emitting Diodes. *Chem. Mater.* **2013**, *25* (22), 4471−4486.
(50) Zink, D. M.; Baumann, T.; Friedrichs, J.; Nieger, M.; Bräse, S. Copper(I) Complexes Based on Five-Membered P∧N Heterocycles: Structural Diversity Linked to Exciting Luminescence Properties. *Inorg. Chem.* **2013**, *52* (23), 13509−13520.
(51) Wallesch, M.; Verma, A.; Fléchon, C.; Flügge, H.; Zink, D. M.; Seifermann, S. M.; Navarro, J. M.; Vitova, T.; Göttlicher, J.; Steininger, R.; et al. Towards Printed Organic Light-Emitting Devices: A Solution-Stable, Highly Soluble $Cu^I$-NHetPHOS. *Chem. − Eur. J.* **2016**, *22* (46), 16400−16405.
(52) Busch, J. M.; Zink, D. M.; Di Martino-Fumo, P.; Rehak, F. R.; Boden, P.; Steiger, S.; Fuhr, O.; Nieger, M.; Klopper, W.; Gerhards, M.; Bräse, S. Highly soluble fluorine containing Cu(I) AlkylPyrPhos TADF complexes. *Dalton Trans.* **2019**, *48* (41), 15687−15698.
(53) Busch, J. M.; Koshelev, D. S.; Vashchenko, A. A.; Fuhr, O.; Nieger, M.; Utochnikova, V. V.; Bräse, S. Various Structural Design Modifications: *para*-Substituted Diphenylphosphinopyridine Bridged Cu(I) Complexes in Organic Light-Emitting Diodes. *Inorg. Chem.* **2021**, *60* (4), 2315−2332.
(54) Volz, D.; Zink, D. M.; Bocksrocker, T.; Friedrichs, J.; Nieger, M.; Baumann, T.; Lemmer, U.; Bräse, S. Molecular Construction Kit for Tuning Solubility, Stability and Luminescence Properties: Heteroleptic MePyrPHOS-Copper Iodide-Complexes and their Application in Organic Light-Emitting Diodes. *Chem. Mater.* **2013**, *25* (17), 3414−3426.
(55) Volz, D.; Chen, Y.; Wallesch, M.; Liu, R.; Fléchon, C.; Zink, D. M.; Friedrichs, J.; Flügge, H.; Steininger, R.; Göttlicher, J.; Heske, C.; Weinhardt, L.; Bräse, S.; So, F.; Baumann, T. Bridging the Efficiency Gap: Fully Bridged Dinuclear Cu(I)-Complexes for Singlet Harvesting in High-Efficiency OLEDs. *Adv. Mater.* **2015**, *27* (15), 2538−2543.
(56) Volz, D.; Wallesch, M.; Grage, S. L.; Göttlicher, J.; Steininger, R.; Batchelor, D.; Vitova, T.; Ulrich, A. S.; Heske, C.; Weinhardt, L.; Baumann, T.; Bräse, S. Labile or Stable: Can Homoleptic and Heteroleptic PyrPHOS−Copper Complexes Be Processed from Solution? *Inorg. Chem.* **2014**, *53* (15), 7837−7847.
(57) He, X.; Zhu, N.; Yam, V. W.-W. Design and synthesis of luminescence chemosensors based on alkynyl phosphine gold(I)−copper(I) aggregates. *Dalton Trans.* **2011**, *40* (38), 9703.
(58) Koshevoy, I. O.; Chang, Y.-C.; Karttunen, A. J.; Shakirova, J. R.; Jänis, J.; Haukka, M.; Pakkanen, T.; Chou, P.-T. Solid-State Luminescence of Au−Cu−Alkynyl Complexes Induced by Metallophilicity-Driven Aggregation. *Chem. − Eur. J.* **2013**, *19* (16), 5104−5112.
(59) Koshevoy, I. O.; Lin, C.-L.; Karttunen, A. J.; Jänis, J.; Haukka, M.; Tunik, S. P.; Chou, P.-T.; Pakkanen, T. A. Stepwise 1D Growth of


https://doi.org/10.1021/acsomega.3c05755
*ACS Omega* 2024, 9, 2220−2233

Luminescent Au(I)−Ag(I) Phosphine−Alkynyl Clusters: Synthesis, Photophysical, and Theoretical Studies. *Inorg. Chem.* **2011**, *50* (6), 2395−2403.
(60) Manbeck, G. F.; Brennessel, W. W.; Stockland, R. A.; Eisenberg, R. Luminescent Au(I)/Cu(I) Alkynyl Clusters with an Ethynyl Steroid and Related Aliphatic Ligands: An Octanuclear $Au_4Cu_4$ Cluster and Luminescence Polymorphism in $Au_3Cu_2$ Clusters. *J. Am. Chem. Soc.* **2010**, *132* (35), 12307−12318.
(61) Wei, Q.-H.; Yin, G.-Q.; Zhang, L.-Y.; Shi, L.-X.; Mao, Z.-W.; Chen, Z.-N. Luminescent $Ag^I$−$Cu^I$ Heterometallic Hexa-, Octa-, and Hexadecanuclear Alkynyl Complexes. *Inorg. Chem.* **2004**, *43* (11), 3484−3491.
(62) Alcock, N. W.; Moore, P.; Lampe, P. A. Crystal and molecular structures of two complexes of diphenyl(2-pyridyl)phosphine (L): [AuCIL] and $[Ag_2Cl_2L_3]$. *Dalton Trans.* **1982**, *7*, 207−210, DOI: 10.1039/DT9820000207.
(63) Inoguchi, Y.; Milewski-Mahrla, B.; Neugebauer, D.; Jones, P. G.; Schmidbaur, H. Synthese und eine Röntgenbeugungsanalyse von Kupfer(I)- und Silber(I)-chlorid-Komplexen. *Chem. Ber.* **1983**, *116*, 1487−1493.
(64) Del Zotto, A.; Zangrando, E. 2-(Diphenylphosphino)pyridine (dppy) as monodentate or bridging ligand in homoleptic silver(I) complexes. Crystal structures of $[Ag(\eta^1\text{-dppy})_4][ClO_4]$ and $[Ag_2(\eta^1\text{-dppy})(\mu\text{-dppy})_2][ClO_4]_2$. *Inorg. Chim. Acta* **1998**, *277* (1), 111−117.
(65) Zink, D. M.; Bächle, M.; Baumann, T.; Nieger, M.; Kuhn, M.; Wang, C.; Klopper, W.; Monkowius, U.; Hofbeck, T.; Yersin, H.; Bräse, S. Synthesis, Structure, and Characterization of Dinuclear Copper(I) Halide Complexes with P∧N ligands Featuring Exciting Photoluminescence Properties. *Inorg. Chem.* **2013**, *52*, 2292−2305.
(66) Busch, J. M.; Ferraro, V.; Bräse, S. Chemotion Repository, 2023. DOI: 10.14272/collection/JMB_2020-08-13.
(67) TURBOMOLE V75 2020: a development of University of Karlsruhe and Forschungszentrum Karlsruhe GmbH, Turbomole GmbH, 2007. https://www.turbomole.org.
(68) Yanai, T.; Tew, D. P.; Handy, N. C. A new hybrid exchange−correlation functional using the Coulomb-attenuating method (CAM-B3LYP). *Chem. Phys. Lett.* **2004**, *393* (1−3), 51−57.
(69) Volz, D.; Zink, D. M.; Bocksrocker, T.; Friedrichs, J.; Nieger, M.; Baumann, T.; Lemmer, U.; Bräse, S. Molecular Construction Kit for Tuning Solubility, Stability and Luminescence Properties: Heteroleptic MePyrPHOS-Copper Iodide-Complexes and their Application in Organic Light-Emitting Diodes. *Chem. Mater.* **2013**, *25*, 3414−3426.
(70) Fackler, J. P.; López, C. A.; Staples, R. J.; Wang, S.; Winpenny, R. E. P.; Lattimer, R. P. Self assembly of isostructural copper(I)-silver(I) butterfly clusters with 2-mercaptothiazoline; syntheses and structures of $(PPh_3)_2Cu_4(C_3H_4NS_2)_4$, $[(C_5H_5N)Cu_4(C_3H_4NS_2)_4]_n$, $(PPh_3)_2Ag_4(C_3H_4NS_2)_4$ and $(PPh_3)_2Ag_2Cu_2(C_3H_4NS_2)_4$. *J. Chem. Soc., Chem. Commun.* **1992**, No. 2, 146−148.
(71) Polgar, A. M.; Zhang, A.; Mack, F.; Weigend, F.; Lebedkin, S.; Stillman, M. J.; Corrigan, J. F. Tuning the Metal/Chalcogen Composition in Copper(I)−Chalcogenide Clusters with Cyclic (Alkyl)(amino)carbene Ligands. *Inorg. Chem.* **2019**, *58* (5), 3338−3348.
(72) Lu, T.; Wang, J.-Y.; Shi, L.-X.; Chen, Z.-N.; Chen, X.-T.; Xue, Z.-L. Synthesis, structures and luminescence properties of amine-bis(N-heterocyclic carbene) copper(i) and silver(i) complexes. *Dalton Trans.* **2018**, *47* (19), 6742−6753.
(73) Zhang, X.; Wang, J.-Y.; Qiao, D.; Chen, Z.-N. Phosphorescent mechanochromism through the contraction of Ag12Cu2 clusters in tetradecanuclear copper−silver acetylide complexes. *J. Mater. Chem. C* **2017**, *5* (34), 8782−8787.
(74) Xu, L.-J.; Zhang, X.; Wang, J.-Y.; Chen, Z.-N. High-efficiency solution-processed OLEDs based on cationic Ag6Cu heteroheptanuclear cluster complexes with aromatic acetylides. *J. Mater. Chem. C* **2016**, *4* (9), 1787−1794.
(75) Hau, S. C. K.; Yeung, M. C. L.; Yam, V. W. W.; Mak, T. C. W. Assembly of Heterometallic Silver(I)−Copper(I) Alkyl-1,3-diynyl Clusters via Inner-Core Expansion. *J. Am. Chem. Soc.* **2016**, *138* (41), 13732−13739.
(76) Jiang, Y.; Guo, W.-J.; Kong, D.-X.; Wang, Y.-T.; Wang, J.-Y.; Wei, Q.-H. Novel electrochemi-/photo-luminescence of Ag3Cu5 heterometallic alkynyl clusters. *Dalton Trans.* **2015**, *44* (9), 3941−3944.
(77) Jarzembska, K. N.; Kamiński, R.; Fournier, B.; Trzop, E.; Sokolow, J. D.; Henning, R.; Chen, Y.; Coppens, P. Shedding Light on the Photochemistry of Coinage-Metal Phosphorescent Materials: A Time-Resolved Laue Diffraction Study of an $Ag^I$−$Cu^I$ Tetranuclear Complex. *Inorg. Chem.* **2014**, *53* (19), 10594−10601.
(78) Chen, Z.-H.; Zhang, L.-Y.; Chen, Z.-N. Structural Characterization and Luminescence Properties of a Triphosphine-Stabilized $Ag_{16}Cu_9$ Heterometallic Alkynyl Cluster. *Organometallics* **2012**, *31* (1), 256−260.
(79) Koshevoy, I. O.; Shakirova, J. R.; Melnikov, A. S.; Haukka, M.; Tunik, S. P.; Pakkanen, T. A. Coinage metal complexes of 2-diphenylphosphino-3-methylindole. *Dalton Trans.* **2011**, *40* (31), 7927.
(80) Olmos, M. E.; Schier, A.; Schmidbaur, H. Diphenyl(1-pyridyl)phosphine Sulfide as a Ligand in Mono-and Binuclear Coinage Metal Complexes. *Z. Naturforsch. B* **1997**, *52* (3), 385−390.
(81) Maini, L.; Mazzeo, P. P.; Farinella, F.; Fattori, V.; Braga, D. Mechanochemical preparation of copper iodide clusters of interest for luminescent devices. *Faraday Discuss.* **2014**, *170*, 93−107.
(82) Ono, S.; Kobayashi, M.; Tomoyose, T. Covalency of noble metal halides. *Solid State Ionics* **2005**, *176* (3−4), 363−366.
(83) Hofbeck, T.; Niehaus, T. A.; Fleck, M.; Monkowius, U.; Yersin, H. P∩N Bridged Cu(I) Dimers Featuring Both TADF and Phosphorescence. From Overview towards Detailed Case Study of the Excited Singlet and Triplet States. *Molecules* **2021**, *26* (11), 3415.
(84) Yersin, H.; Leitl, M. J.; Czerwieniec, R.*TADF for Singlet Harvesting: Next Generation OLED Materials Based on Brightly Green and Blue Emitting Cu(I) and Ag(I) Compounds*, Proceedings of SPIE, Organic Light Emitting Materials and Devices XVIII, 2014.
(85) Osawa, M.; Hashimoto, M.; Kawata, I.; Hoshino, M. Photoluminescence properties of TADF-emitting three-coordinate silver(I) halide complexes with diphosphine ligands: a comparison study with copper(I) complexes. *Dalton Trans.* **2017**, *46*, 12446.
(86) Henary, M.; Zink, J. I. Luminescence from the chair and cube isomers of tetrakis[(triphenylphosphine)iodosilver]. *Inorg. Chem.* **1991**, *30*, 3111−3112.
(87) Vogler, A.; Kunkely, H. Photoluminescence of tetrameric silver(I) complexes. *Chem. Phys. Lett.* **1989**, *158*, 74−76.
(88) Teo, B.-K.; Calabrese, J. C. Stereochemical systematics of metal clusters. Crystallographic evidence for a new cubane. dblharw. chair isomerism in tetrameric triphenylphosphine silver iodide, $(Ph_3P)_4Ag_4I_4$. *Inorg. Chem.* **1976**, *15* (10), 2474−2486.


https://doi.org/10.1021/acsomega.3c05755
*ACS Omega* 2024, 9, 2220−2233